07 September, 2007

CHAPTER-5

Uranium-and Thorium- Series Nuclides as Tracers of Submarine Groundwater Discharge

M.A. Charette[1], W. S. Moore[2] and W.C. Burnett[3]

[1]Department of Marine Chemistry and Geochemistry,

Woods Hole Oceanographic Institution, Woods Hole, MA 02543, USA

[2]Department of Geological Sciences, University of South Carolina, Columbia, SC 29208, USA

[3]Department of Oceanography, Florida State University, Tallahassee, FL 32306, USA

CHAPTER-5

Uranium-and Thorium-Series Nuclides as Tracers of Submarine Groundwater Discharge

M.A. Charette, W. S. Moore and W.C. Burnett

CHAPTER-5

Uranium-and Thorium-Series Nuclides as Tracers of Submarine Groundwater Discharge

1. Introduction

Subsurface discharge of water from coastal aquifers, called submarine groundwater discharge (SGD), has been recognized as an important component of the hydrological cycle. This discharge includes meteoric water from land drainage as well as seawater that has entered coastal aquifers. We follow Burnett et al. (2003) in defining SGD as any and all flow of water on continental margins from the seabed to the coastal ocean, regardless of fluid composition or driving force. Our definition does not include hydrothermal discharges, which are discussed in another chapter (Cochran and Kadko, this volume).

Studies of SGD usually classify all saturated permeable materials in the coastal zone and on the continental shelf as aquifers. Thus, advective flow through such materials into the ocean is considered SGD. Coastal aquifers often consist of complicated arrays of confined, semi-confined, and unconfined systems (Fig. 1). Simple hydrologic models do not consider the anisotropic nature of coastal sediments, dispersion, and tidal pumping. Moreover, cycling of seawater through the coastal aquifer may be driven by the flow of freshwater from coastal uplands (Cooper, 1959; Destouni and Prieto, 2003). As freshwater flows through an aquifer driven by an inland hydraulic head, it can entrain seawater from the salty underlying aquifer. Concurrent peaks in the annual cycles of evapotranspiration and precipitation can result in yearly maximum recharge with subsequent, although delayed, seasonal changes in discharge rates (Michael et al., 2005). Superimposed upon this land driven circulation are a variety of marine-induced processes that result in flow into and out of the seabed even in the absence of a hydraulic head. Such “subterranean estuaries” (Moore, 1999) are characterized by biogeochemical reactions that influence the transfer of nutrients, carbon, and metals to the coastal zone in a manner similar to that of surface estuaries (Nixon et al., 1986; Charette and Sholkovitz, 2002; Talbot et al., 2003).

SGD is increasingly being recognized as an important factor in the understanding and sustainable management of coastal fresh water aquifers, especially in many highly populated areas of the world. In addition, SGD is a significant pathway for transfer of materials between the land and the sea (Moore, 1999; Charette and Sholkovitz, 2002). For example, SGD is known to supply essential nutrients and trace metals to coastal ocean ecosystems (Valiela et al., 1978, 1990, 1992, 2002; Johannes, 1980; D'Elia et al., 1981; Capone and Bautista, 1985; Capone and Slater, 1990; Corbett et al., 1999, 2000; Krest et al., 2000; Crotwell and Moore, 2003; Moore et al., 2006; Windom et al., 2006; Burnett et al., 2007). In some cases SGD may result in contamination of the near-shore marine environment from land-based activities (Oberdorfer et al., 1990; Lapointe et al., 1990; LaRoche et al., 1997; Boehm et al., 2004). Additionally, SGD may remove certain components (e.g., uranium) from seawater during circulation through coastal aquifers (Charette and Sholkovitz, 2006; Moore and Shaw, submitted). Thus, SGD and related processes may be important as both a source and a sink in geochemical cycles. As we learn more about SGD and subterranean aquifers, we recognize how significant these processes are to the coastal ocean.

Many researchers have applied a variety of methods to estimate SGD (see Burnett et al., 2006 for a review). Estimation of SGD is complicated due to the fact that direct measurements over large temporal and spatial scales are not possible by conventional methods. Measurements of a range of isotopic tracers at the aquifer-marine interface and in the coastal ocean provide a means to obtain integrated flux estimates of discharge not possible by non-nuclear methods (Moore, 1999). The large spread in the global estimates for SGD fluxes illustrates the high degree of variability and uncertainty of present estimates. It should be noted that the estimates based on water balance considerations and some models usually provide only the freshwater fraction of the total hydrologic flow. Recirculated seawater and saline groundwater fluxes are often volumetrically important and may increase these flows substantially.

In cases of freshwater fluxes, chemical anomalies such as salinity are useful for estimation of SGD. However, in cases of brackish and saline SGD fluxes, which in many cases have more impact on the coastal environment, isotopes have distinct advantages over chemical techniques. Investigations using a combination of stable isotopes, long-lived, and short-lived

radioisotopes along with other complementary techniques allow various aspects of SGD related coastal hydrology to be studied.

Isotopic measurements such as ^{222}Rn, ^{226}Ra, ^{228}Ra, ^{224}Ra, ^{223}Ra, ^{87}Sr, ^{3}He, ^{4}He, ^{3}H, ^{14}C, ^{234}U and ^{238}U among others can serve as key indicators of fluxes across the groundwater/marine interface. Of these, the U-Th series decay products ^{222}Rn, ^{226}Ra, ^{228}Ra, ^{224}Ra, and ^{223}Ra (Appendix, Figs. 1-3) have been used the most extensively (Burnett et al., 1990, Ellins et al., 1990; Moore and Shaw, 1998; Corbett et al., 1999; Swarzenski et al., 2001; Garrison et al., 2003; Krest and Harvey, 2003; Kim et al., 2003; Breier et al., 2005; Moore and Wilson, 2005; Dulaiova et al., 2006; Paytan et al, 2006 and others referenced herein). These isotopic techniques enable large-scale estimates of various components of SGD, allowing detailed studies on the processes involved. Most of the presently applied U-Th series isotope techniques are of potential use in a variety of SGD investigations. Additionally, new isotope techniques for *in situ* study are under development including underwater gamma spectrometry and continuous radon monitoring (Povinec et al., 2001; Dulaiova et al., 2005). These techniques may be more useful for location of SGD discharges rather than estimation of their magnitudes.

2. How U-Th isotopes are used to quantify SGD

One major limitation in quantifying SGD to the coastal zone on a global scale has been the lack of reliable techniques for determining the flux at specific sites. In this regard, a number of U-Th series isotopes have become popular tools for quantifying SGD (e.g., Cable et al., 1996a; Moore, 1996). A primary desirable characteristic of an isotopic tracer of SGD is that it has a unique or dominant source in groundwater, is distinctly different from that in ambient seawater and that its contributions from other vectors (e.g., river water, rainfall) to the region of study are small and/or quantifiable. The isotope could be enriched in groundwater relative to seawater, in which case the groundwater would be a source of isotope to the coastal zone. The opposite case is also applicable, for example when an isotope is enriched in seawater but depleted in groundwater (e.g., uranium). We discuss this specialized case in section 5.

In order to quantify SGD using a U-Th series isotope, generally a box model approach is used (Fig. 2). By definition, non-point source fluxes such as SGD are notoriously difficult to

quantify. Thus, a "flux by difference" approach is required, whereby all quantifiable fluxes are subtracted from the flux required to support the inventory of the isotope with the residual flux being attributed to SGD. Besides SGD, there are five main pathways for enrichment or removal of these nuclides in the coastal ocean that must be considered:

Enrichment

1 Riverine discharge. This includes isotopes carried by rivers not only in dissolved form, but also those released by suspended sediments.
2. Release from the bottom sediments to pore waters and subsequent supply by molecular diffusion, bioturbation, and erosion (sediment resuspension). In most study areas, there are distinct zones from which SGD originates (e.g., a narrow band that follows the shoreline or offshore breaches in confining units). However, release of isotopes from bottom sediments (without SGD) must also be considered as a potential source.

Removal

1. Exchange with open ocean waters. Enrichments of a U-Th series isotope in coastal waters due to SGD can vary widely from only 10% greater than seawater (e.g., Boehm et al., 2006) to a factor of 100 or higher (e.g., Burnett and Dulaiova, 2003). Exchange of these coastal waters with the open ocean will effectively transfer nuclides from coast to open sea.
2. Atmospheric evasion. This applies only to radon and results in its transfer from surface waters to the atmosphere. This is often a significant loss term, except in special cases.
3. Radioactive Decay. This term can typically be ignored for isotopes with half-lives longer than ~1 year due to the relatively short residence time of water within the defined box (e.g., an estuary or coastal ocean).

Scavenging/biological uptake which can affect the budget is another removal process. For Ra, which is commonly used as a natural tracer (Section. 3) to estimate SGD, this process is assumed negligible relative to other removal terms in the coastal ocean. Balancing these enrichment and removal terms gives (neglecting physical mixing and bioturbation of sediments):

$$\frac{\partial A}{\partial t} = \underbrace{\left[\frac{A - A_{ocn}}{T_w}\right]}_{Oceanic\_Source} - \underbrace{\left[\frac{F_{riv}A_{riv} + F_{riv}A_{desorb}}{V}\right]}_{Riverine\_Source} - \underbrace{\left[\phi D_s\left(\frac{\partial^2 A_{sed}}{\partial z^2_{sed}}\right) + \omega\left(\frac{\partial A_{sed}}{\partial z_{sed}}\right)\right]}_{Benthic\_Advection\_Diff.\_Source}$$
$$+ \underbrace{\left[\frac{e_g\left(A - A_{atm}\right)}{z_{wc}}\right]}_{Atmospheric\_Evasion} + \underbrace{\left[\lambda A\right]}_{Decay} \quad (1)$$

where A is the average activity (dpm m^{-3}) of the isotope within the study area, A_{ocn} is the isotope activity of the ocean water that exchanges with the study area, z_{wc} is the water column or mixed layer depth (m), V is the water volume of the study area (m^3), T_w is the water residence time (days), F_{riv} is the volumetric water flux from rivers (m^{-3} d^{-1}), A_{riv} is the average fresh water endmember activity for the river, A_{desorb} is the suspended sediment activity available for release to the water phase, ϕ is the sediment porosity (unitless), D_s is the isotope (e.g. ^{226}Ra) diffusion coefficient in pore water of sediments (m^2 d^{-1}), $\partial A_{sed}/\partial z$ is the vertical gradient of the isotope concentration in pore waters of the sediments, ω is the advective velocity of pore water from the sediments (SGD; m d^{-1}), e_g is the air-sea piston velocity (m d^{-1}), A_{atm} is the isotope concentration in the marine boundary layer, and λ is the decay constant (d^{-1}). The relative importance of these sources and sinks will vary according to the characteristics of the study site and the isotope used. In the following, specific applications of selected U-Th isotopes in studies of SGD are discussed.

3. Radium

3.1 Applications to estimate SGD

Radium isotopes have proven to be useful tracers of total SGD in many environments on both small and large scales from salt marshes (Rama and Moore, 1996; Krest et al., 2000; Charette et al., 2003) to estuaries (Charette et al., 2001; Kelly and Moran, 2002; Yang et al., 2002) and to the continental shelf (Moore, 1996; Kim et al., 2005). Moore (1996) first reported linking the large-scale input of radium isotopes to the ocean via groundwater discharge in a study conducted along the South Atlantic Bight (US).

In general, the approach of Moore (1996) to calculate SGD is the method still in use. In this work, the initial step was a survey of ^{226}Ra activities on several shore perpendicular transects

off the coast of South and North Carolina (Fig. 3) and subsequent modeling of the data. Five potential sources of ^{226}Ra were identified: (1) ocean water, (2) river water, (3) desorption from river-borne particles, (4) erosion of terrestrial sediments along the shoreline, and (5) groundwater. The flux by difference approach (eqn.1) with the assumption of steady state and negligible radioactive decay ($t_{1/2}$ =1600 y) was then applied to the radium data from the inner shelf region:

$$F_{SGD} = \frac{\left(\left[\frac{(A - A_{ocn})}{T_w}\right] - \left[\frac{F_{riv}A_{riv} + F_{riv}A_{desorb}}{V}\right] - \left[\phi D_s\left(\frac{\partial^2 A_{sed}}{\partial z^2_{sed}}\right)\right]\right) z_{wc}}{A_{gw}} \qquad (2)$$

where F_{SGD} is the per unit area fluid flux via SGD (m^3 m^{-2} d^{-1} or m d^{-1}) and A_{gw} is the groundwater endmember radium activity. Given that ^{226}Ra is produced by decay of ^{230}Th, the regeneration time for ^{226}Ra in the sediments is very long, on the order of hundreds to thousands of years. The sediment diffusion source was therefore considered negligible. Using literature estimates of residence time, riverine discharge/suspended sediment load, and the activity of desorbable ^{226}Ra on riverine particles, Moore (1996) determined that only ~50% of the ^{226}Ra inventory could be accounted for by the first four sources mentioned above. Finally, using an estimate of groundwater ^{226}Ra, it was inferred that the total (fresh + saline) groundwater flux to this region of the coastline was on the order of 40% of the river water flux.

In a subsequent paper, Moore (2000a) described a more streamlined approach for calculating the flux, one that involved the use of the short-lived Ra isotopes and does not require a box model per se. Values of the K_h (horizontal eddy diffusion coefficient; see section 1.2.2.) were used in conjunction with the cross shelf ^{226}Ra activity gradient ($\partial A/\partial x$) to estimate offshore fluxes:

$$F_{SGD}A_{gw} = \left[K_h\left(\frac{\partial A}{\partial x}\right)\right] \times (z \bullet L) \qquad (3)$$

where z is the surface layer depth (m) over which Ra is transported and L is the shoreline length (m). Measurements of the ^{226}Ra activity in submarine groundwater coupled with the computed offshore fluxes yield estimates of the discharge of SGD into the coastal ocean. Companion analyses of other parameters can be used to estimate the flux of other solutes entering the ocean via SGD (e.g., nutrients, trace metals).

Salt marshes have been the focus of numerous studies on Ra as a tracer of SGD. Rama and Moore (1996) were the first to determine that fluxes of ^{226}Ra and ^{228}Ra from a salt marsh (North Inlet, S.C.) were much larger than could be supported by the decay from Th parents in the surface sediments. A two-box model was used to describe water and sediment exchange between a deep sediment layer (box 1) and a surface sediment layer (box 2). Charette et al. (2003) examined SGD in the Great Sippewissett Marsh, MA, via interpretation of a unique set of radium data spanning nearly two decades (1983, 1985, 1999, 2001). Despite higher average salinity, activities of ^{226}Ra and ^{228}Ra were remarkably higher in 1999 than in the other years. The authors suggested that the differences could be accounted for by more SGD with a greater component of recirculated seawater due to enhanced groundwater-seawater interaction during 1999, which was one the driest years on record during the 20-year study period.

The existence of four naturally-occurring radium isotopes makes Ra particularly useful for quantifying multiple sources of SGD, such as fluid originating from confined versus surficial aquifers (Crotwell and Moore, 2003; Moore, 2003; Charette and Buesseler, 2004). This approach is made possible through two primary mechanisms. First, aquifers with different principal mineral or sediment types can have different relationships among uranium (^{238}U -> ^{226}Ra; ^{235}U -> ^{223}Ra) and thorium (^{232}Th -> ^{228}Ra -> ^{224}Ra) series isotopes. For example, aquifers with a predominance of carbonate minerals (e.g., karst) are enriched in U relative to Th, and therefore in U-series daughters (e.g. ^{226}Ra >> ^{228}Ra). Secondly, seawater circulation through an aquifer can supply/deposit sediments, which are the ultimate source of Ra isotopes in groundwater, enriched in the shorter-lived isotopes and depleted in the longer-lived isotopes due to the relative differences in rates of ingrowth from their thorium parents (e.g. ^{228}Ra >> ^{226}Ra; Hancock and Murray, 1996).

Moore (2003) used the $^{228}Ra/^{226}Ra$ AR (activity ratio) to distinguish groundwater derived from the carbonate upper Floridan Aquifer (UFA) vs. the clastic surficial aquifer (SA) in samples collected from the Gulf coast of Florida. The results showed that most surface water samples fell along a mixing line having a $^{228}Ra/^{226}Ra$ AR=2.5, indicating a surficial aquifer source (Fig. 4). However, some offshore samples fell off this trend and toward a sample from an artesian well in the UFA. The low $^{228}Ra/^{226}Ra$ AR in the offshore plume indicated that the deeper aquifer was flushed slower than the near shore aquifer and/or that the $^{232}Th/^{230}Th$ AR of the solids was lower in the UFA. The $^{228}Ra/^{226}Ra$ AR in springs in the area showed that they were also influenced by the UFA source. Based on these observations, Moore (2003) developed a 3-endmember mixing model to assess the relative contributions of water from the open Gulf, the offshore UFA, and the nearshore SA in the surface water samples. A result of the model was the presence of a significant and variable UFA component in the surface water. Charette and Buesseler (2004) used a similar approach to distinguish between salt marsh derived groundwater and a shallow semi-confined aquifer in the Chesapeake Bay region. This study highlighted salt marshes as being particularly suited to the 3-endmember SGD approach, since the pore waters of the marsh sediments, which are repeatedly flushed on tidal time scales, are highly enriched in ^{228}Ra relative to ^{226}Ra compared with typical aquifer pore waters. In general, salt marsh $^{228}Ra/^{226}Ra$ activity ratios are often in the range of 10-20 (Rama and Moore, 1996; Krest et al., 2000; Charette and Buesseler, 2004).

Distinct $^{228}Ra/^{226}Ra$ ARs in groundwater endmembers were also observed on the southern coast of Sicily (Moore, 2006). Springs from a limestone aquifer discharging on the beach and just offshore had much lower $^{228}Ra/^{226}Ra$ AR than did shallow wells on the beach. Samples collected in the nearshore zone as well as samples collected in bags fixed to benthic chambers (seepage meters) fell between the isotopic compositions of these sources. Again the 3-endmember model was able to resolve these sources.

SGD in river-dominated areas can be significant in some cases but difficult to evaluate because of the high river-derived fluxes. Dulaiova et al. (2006) used ^{222}Rn and radium isotopes (^{223}Ra, ^{224}Ra, ^{226}Ra, ^{228}Ra) to assess the magnitude of groundwater discharge in the Chao Phraya River and estuary (Gulf of Thailand). The isotopic results suggested that there are at least three

different sources of these tracers in the estuary: river water, seawater, and groundwater. They estimated the extent of each input via a mixing model using ^{222}Rn, ^{223}Ra, and ^{224}Ra activities and ^{224}Ra:^{223}Ra ratios. Their analysis showed that the largest groundwater outflow occurs near the mouth of the river. The estimated groundwater inputs represented about 20% of the river flow during low flow conditions (January) and 4% during high flow (July).

Along high-energy coastlines, wave run-up and tidal pumping are often the driving force behind SGD. Boehm et al. (2004, 2006) used Ra isotopes to study SGD in one such environment: Huntington Beach in Southern California. Though the degree of enrichment in the groundwater of the beach face was low, Boehm et al. (2004) showed that the two short-lived Ra isotopes as measured in the surf zone fell along a mixing line between offshore waters and the groundwater endmember. The flux estimates based on ^{223}Ra and ^{224}Ra were supported by a later analysis of ^{226}Ra at this location (Boehm et al., 2006) and by the results of a numerical model. Boehm et al. (2006) concluded that SGD consisted primarily (~75%) of recirculated seawater driven by the tides and wave action.

3.2 Applications for determination of water residence times

As discussed earlier, knowledge of water residence time (T_w) is required for quantifying SGD using the flux by difference approach. The large-scale input of radium isotopes along the coastline and the boundaries of estuaries is akin to a purposeful tracer release, with the short-lived radium isotopes providing the rate of dispersion based on their decay as they mix away from the source (Ku and Luo, this volume). Both residence time and age are used to describe how long water remains in an estuary. One definition of residence time is "the time it takes for any water parcel to leave a given water body through its outlet to the sea", usually relative to an arbitrary reference point within the system (Monsen et al., 2002). On the other hand, age is defined as the time a water parcel has spent since entering the estuary through one of its boundaries. Often these two measures of time yield consistent results. Ra isotopes have been used to determine the time since the water parcel was last in contact with the boundary (input via SGD). This time, T_w, may be derived (Moore, 2000b; Charette et al., 2001) based on the relation between ^{223}Ra/^{228}Ra in groundwater and in the estuary:

$$\left[\frac{ex^{223}Ra}{ex^{228}Ra}\right]_{obs} = \left[\frac{ex^{223}Ra}{ex^{228}Ra}\right]_{i} e^{-\lambda_{223}T_w} \quad (4)$$

ex designates the excess activity of the isotope obtained by subtracting their open ocean concentrations from the observed activities in estuaries/coasts. This is done to determine the concentration of Ra isotopes resulting from near shore supply. The $(ex^{223}Ra/ex^{228}Ra)_i$ is the activity ratio of the end-member groundwater and $(ex^{223}Ra/ex^{228}Ra)_{obs}$ is the activity ratio in the sample(s) of interest. This method assumes that (i) the initial $ex^{223}Ra/ex^{228}Ra$ ratio is constant (Moore, 2000b) and (ii) normalization with ^{228}Ra provides corrections for changes in ^{223}Ra concentration which may result from processes other than radioactive decay (e.g., mixing). As T_w is generally quite short, the decay of ^{228}Ra can be neglected. In practice, the supported activity of ^{223}Ra in the open ocean is essentially 0 such that $ex^{223}Ra = {}^{223}Ra$. This is in contrast with ^{228}Ra, which is measurable in most open ocean basins. Finally, ^{224}Ra can also be used in place of ^{223}Ra, however, because of its short half life (3.66 d) it is applicable only to waters with $T_w \leq 10$ days)

The greatest uncertainty with this method is the inherent variability in the endmember (i.e., groundwater) $ex^{223}Ra/ex^{228}Ra$ ratio (see section 2.4 for further discussion on this topic). In addition, this model assumes that radium is added to the water only near the shoreline and that after the water parcel leaves the coast there is no further addition. This requirement is unlikely to be met in estuaries and salt marshes, where radium additions from sediments and groundwater are continuous; therefore in these cases, T_w estimates using this method would be lower-limits. To solve this problem in estimating ages in these systems, Moore et al. (2006) and Hwang et al. (2005a) used a different approach as described below.

If the system under study is in steady state, then radium additions are balanced by its losses. Additions include radium fluxes from sediment, river, and groundwater; losses are due to mixing and, in the case of ^{223}Ra and ^{224}Ra also by radioactive decay. The balance equation for ^{224}Ra can be written as:

$$F^{224}Ra = I^{224}Ra\left(\lambda_{224} + \frac{1}{T_w}\right) \quad (5)$$

where F ^{224}Ra is the total flux (dpm m^{-2} d^{-1}) of ^{224}Ra to the system, I ^{224}Ra is its inventory (dpm m^{-2}), λ_{224} is its decay constant (d^{-1}), and T_w is the apparent age (d) of water in the system. A similar equation can be written for ^{228}Ra; however, because its half-life is 5.7 years, the effect of decay can be ignored.

$$F^{228}Ra = I^{228}Ra\left(\frac{1}{T_w}\right) \tag{6}$$

Dividing equation 5 by equation 6 and rearranging:

$$T_w = \frac{\left[F\left(^{224}Ra/^{228}Ra\right) - I\left(^{224}Ra/^{228}Ra\right)\right]}{I\left(^{224}Ra/^{228}Ra\right)\lambda_{224}} \tag{7}$$

In this case F (^{224}Ra/^{228}Ra) is the ^{224}Ra/^{228}Ra activity ratio (AR) of the input into the system and I (^{224}Ra/^{228}Ra) is the ^{224}Ra/^{228}Ra AR of the system. The application of this model requires precise knowledge of the ^{224}Ra/^{228}Ra AR of input. This value can be determined by measuring the ratio in shallow groundwater in areas of discharge identified by infrared imaging or other techniques. Another approach is to collect data from the pore water of shallow permeable sediments and plot ^{224}Ra vs. ^{228}Ra to determine the average activity ratio of the pore water supplying the two isotopes to the system. Lastly, the ^{224}Ra/^{228}Ra AR is useful on time scales appropriate to the ^{224}Ra half-life (up to ~10 days). In cases where ages are expected to be on the order of weeks, a similar equation based on ^{223}Ra (λ = 0.0608 day^{-1}) would be more appropriate.

3.3 Seasonality in SGD

In many temperate and tropical regions, seasonal patterns in the water cycle play an important role in modulating SGD (Cable et al., 1997; Michael et al., 2005). An early suggestion that seasonality might be important in SGD-derived inputs of radium came from Moore (1997), who observed high fluxes of radium from the Ganges-Brahmaputra River system during a period of low river discharge. This led to the suggestion that during high river discharge, coastal aquifers are recharged with freshwater, a situation where the distribution coefficient (K_d) for Ra

is high and can lead to its sorption to aquifer solids. Subsequently, during low river discharge, saline groundwater intrudes into the aquifer and desorbs the accumulated radium, which is returned to sea via SGD. Indeed, Krishnaswami et al. (1991), in their studies of brines showed that the retardation factor for Ra is inversely correlated with salinity.

Kelly and Moran (2002) looked at seasonal changes in SGD by conducting a monthly time series of radium isotopes in a well-mixed estuary (Pettaquamscutt River, RI). The pattern of SGD input to the estuary, based on ^{226}Ra and ^{228}Ra input, followed the sinusoidal pattern of water table elevation for watersheds in temperate climates, with maximum discharge in late spring, minimum discharge in early winter (Fig. 5).

Moore et al. (2006) determined the SGD fluxes for the Okatee River estuary (Georgia, USA) using ^{226}Ra, ^{228}Ra, and ^{224}Ra. The highest fluxes occurred in the summer and the lowest in winter. The summer fluxes were higher by a factor of four compared to that in the winter. Similar seasonal differences in SGD fluxes have been inferred from studies that reported differences in radium fluxes (Moore, 1987; Bollinger and Moore, 1993). Recently Michael et al. (2005) reported SGD fluxes that were out of phase with the seasonal recharge cycle due to lags of several months between peak recharge and the arrival of this water at the coast.

3.4 Processes controlling end member Ra concentrations

The chemical behavior of radium is such that its K_d decreases significantly in saline environments, mainly due to cation exchange processes (Li and Chan, 1979; Krishnaswami et al., 1991). Thus, radium is usually enriched (relative to surface water) in brackish to saline groundwater; fresh (low ionic strength) SGD that bypasses the regional mixing zone between fresh and saline groundwater (Fig. 1) often will not acquire a significant radium signal and hence may not be quantified (Mulligan and Charette, 2006). However, this is not always the case. Moore (2003, 2006) measured high ^{226}Ra activity in fresh artesian waters on the Florida Gulf coast and Donnalucatta, Sicily, as did Charette and Buesseler (2004) in fresh groundwater from a limestone aquifer in eastern Virginia.

Variability in groundwater radium for a given study site can often span an order of magnitude or more (Moore, 1996; Abraham et al., 2003). Given that this value is used to quantify SGD, this variability represents the greatest uncertainty in Ra-derived estimates of SGD. Processes controlling the cycling of radium in coastal groundwater include: (1) ion exchange reactions with seawater, and (2) the redox cycle of Mn and Fe, (3) weathering of Ra-bearing minerals, and (4) ingrowth from decay of ^{230}Th.

In Waquoit Bay, (Massachusetts, USA) groundwater ^{226}Ra displays a non-conservative distribution between fresh and saline groundwater, such that the highest activities observed occur above a salinity of 25 (Fig. 6). The groundwater ^{226}Ra activities are of the orders of magnitude higher than the bay water (Charette et al., 2001), a pattern in contrast to the typical distribution of radium in surface waters, where activities often peak at intermediate salinity due to a desorption reaction related to ion exchange (Moore et al., 1995). One simple explanation would be an increased ^{226}Ra source with increasing depth and distance from shore, a function of either (1) higher sediment ^{230}Th activities or (2) a decrease in grain size, releasing trapped radium and allowing more surface area available for desorption. Given radium's strong affinity for Mn (hydr)oxides, the Mn redox cycle may also play a role in coastal groundwater Ra cycling. A good analogy would be the control of Fe (hydr)oxides and the "iron curtain" on phosphorous cycling in subterranean estuaries (Charette and Sholkovitz, 2002). A second notable feature of the ^{226}Ra data is that groundwater activities were on average significantly higher during the summer (June) sampling period, which supports the idea of seasonal control on Ra release, as discussed earlier.

Given the many complex processes that control Ra activities in coastal aquifers and permeable sediments, there is not yet a completely satisfactory approach to determine the endmember Ra for the purpose of estimating SGD. However, it is recommended that samples be collected near the point of discharge; the fluid sampled from inland wells may not be representative of the fluid that is supplying Ra to the coastal zone. This sampling can be performed with permanent wells or hand-driven piezometers (Charette and Allen, 2006). The fluid from seepage meters may also be used, though in some cases the headspace water may dilute the discharging groundwater. In either case, natural variability in the endmember activities

(Fig. 6) requires that a large number of samples be collected to reduce uncertainty on the average.

3.5 Applications to determine nutrient flux

Perhaps the most common use of the Ra SGD tracer has been its application to determine nutrient fluxes. The importance of coastal groundwater discharge in delivering dissolved nutrients, such as nitrate and phosphate, to coastal waters has often been overlooked, primarily because it is difficult to estimate (Johannes, 1980; Nixon et al., 1986; Simmons, 1992). The problem lies in the fact SGD had been difficult to quantify using traditional methods such as seepage meters since the discharge is often patchy and may vary with time. Even if SGD is modest, dissolved nutrient concentrations in groundwater may be sufficiently high to have a significant impact on the nutrient budgets for receiving waters. In addition, even in the case that groundwater/pore water may not be overly enriched in nutrients, SGD may enhance the flux of nutrients regenerated in the surface sediments into the overlying water columns.

The approach via the radium tracer is relatively simple: the nutrient flux is the product of the Ra-derived SGD flux and the average nutrient concentration in the groundwater endmember. However, many of these calculations do not take into account the potential nutrient transformations that may occur in the subterranean estuary. These include such processes as denitrification, sorption of phosphorous to Fe (hydr)oxides, and desorption of ammonium during seawater intrusion. Studies should therefore focus on sampling wells located as close to the location of discharge as possible.

In a study of the North Inlet (South Carolina, USA) salt marsh system, Krest et al. (2000) used the two long-lived Ra isotopes to determine mass balances for two nutrients, inorganic nitrogen and phosphorus. The SGD-derived nutrient fluxes were such that the saline aquifer flux beneath the marsh was in balance with net productivity in the marsh and export of dissolved nutrients to offshore waters. In addition, it was determined that this latter flux, when extrapolated to include other salt marshes along the coast, could be on par with riverine nutrient inputs to the coastal zone.

Charette et al. (2001) applied radium isotopes in the study of nitrogen discharge from a coastal aquifer on Cape Cod where groundwater DIN levels were typically four orders of magnitude greater than in the surface waters of Waquoit Bay (Massachusetts, USA). Though both DIN and radium were elevated in groundwater, the relative magnitude of enrichment was spatially variable over short distances. Comparison of SGD-derived fluxes of "new" nitrogen with published primary productivity estimates (Valiela et al., 1992) suggested that this nitrogen was utilized by phytoplankton in the bay during the summer but exported offshore during winter.

Moore et al. (2002) examined SGD-derived nutrient fluxes on the southeastern US continental shelf using data from six monitoring wells located 15-20 km offshore. Some of the wells were set into a high permeability zone (HPZ) located ~2 m beneath the seabed; others were set into sand. A semi-diurnal cycle in temperature within the HPZ suggested that fluid was being exchanged with the overlying water column. The wells had a range of ^{226}Ra activity with a strong relationship between ^{226}Ra and both total dissolved nitrogen (TDN) and total dissolved phosphorous (TDP) (Fig. 7). Moore et al. (2002) combined the TDN/^{226}Ra and TDP/^{226}Ra ratios in the wells with earlier estimates of ^{226}Ra flux to determine N and P fluxes from the seabed. When combined with the SGD fluxes to salt marshes estimated by Krest et al. (2000), the resulting N and P fluxes from SGD clearly exceeded the sum of both riverine and atmospheric sources. Using the Ra approach, Kim et al. (2005) determined that SGD-derived silicate fluxes to the Yellow Sea were on the same order of magnitude as the Si flux from the Yangtze River, the fifth largest river in the world. Burnett et al. (2007) determined that SGD fluxes of N and P to the Upper Gulf of Thailand were 40-70% of the fluxes from the Chao Phraya River. Considering that this river flows through the megacity of Bangkok, where it receives nutrients from industrial and domestic sources, this finding is especially significant.

Hwang et al. (2005a) took a unique approach to quantifying SGD and associated nutrient fluxes for Yeoja Bay, Korea. They solved simultaneous mass-balance equations for ^{226}Ra, ^{223}Ra, and dissolved silicate, which like Ra, also tends to have a strong groundwater source. The resulting fluxes were an order of magnitude higher than previous studies in similar hydrogeologic environments suggesting that SGD was likely to play a significant role in the annual formation of harmful algae blooms in the offshore area of Yeoja Bay. Using the two

short-lived Ra isotopes applied to the flux-by-difference approach, Paytan et al. (2006) determined that SGD was a significant source of "new" nitrogen and other groundwater associated contaminants to coral reef ecosystems, regardless of the hydrogeologic characteristics of the fringing coastline.

The strong correlation between N and P and ^{226}Ra in the groundwater wells reported by Moore et al. (2002) implies mixing between enriched and depleted endmembers. However, it is not always the case that nutrients and radium are so tightly coupled. The wells analyzed by Moore (2002) were offshore, where the source for nutrient enrichment is likely to be regenerated from sediment or organic carbon mineralization. In populated coastal systems where anthropogenic input of nutrients to groundwater can occur, the sources of nutrients and radium are usually independent. In such cases, groundwater is "labeled" with radium prior to discharge (during fresh-saline groundwater interaction), which makes the Ra-derived SGD tracer technique feasible.

3.6 Applications to metal flux

Several studies indicate that groundwater may also contribute significant fluxes of trace metals to the oceans (Shaw et al., 1998; Charette and Buesseler, 2004; Windom et al., 2006). Charette and Buesseler (2004) used radium isotopes to investigate the role of SGD in the delivery of copper to the Elizabeth River estuary, VA, which is characterized by a heavily urbanized and industrialized watershed that includes the largest naval port in the world (Norfolk Naval Base). They estimated that Cu derived from SGD was comparable with estimates of diffusive flux from benthic chambers. This highlighted the importance of advective inputs of trace metals through permeable sediments (as derived from SGD) in addition to diffusive inputs from fine grained, less permeable sediments in coastal areas.

Windom et al. (2006) reported a study of coastal waters of southern Brazil using radium isotopes to quantify SGD advecting through coastal permeable sands into the Atlantic. In this study it was also observed that the concentration of dissolved iron in these beach pore waters were high, implying that there can be large SGD Fe fluxes to coastal waters. Using mixing rates derived from the short lived Ra isotopes and dissolved Fe measurements in the coastal waters,

they calculated that the cross-shelf Fe flux from this 240 km coastline is equivalent to about 10% of the atmospheric flux to the entire South Atlantic Ocean.

4. Radon

4.1 Applications to SGD

The utility of ^{222}Rn as a tracer of SGD has been demonstrated in a wide range of environments from coastal embayments to the coastal ocean (Cable et al., 1996a; Corbett et al., 1997). The very large enrichment of ^{222}Rn concentration in groundwater over surface waters (often 1000-fold or greater), its unreactive nature, and short half-life ($t_{1/2}$ = 3.83 d) make ^{222}Rn an excellent tracer to identify areas of significant groundwater discharge.

The approach for quantifying SGD using ^{222}Rn is similar to radium (^{226}Ra), except for a few key differences: (1) ^{222}Rn loss to the atmosphere must be accounted for in many situations (Church and Sarin, this volume), (2) there is no significant source from particles in rivers, and (3) decay must be accounted for owing to its relatively short half-life. Using the steady state flux by difference approach, equation (1) takes the form:

$$F_{SGD} = \frac{\left[\frac{(A - A_{ocn})z_{wc}}{T_w}\right] - \left[\phi D_s \left(\frac{\partial A_{sed}}{\partial z_{sed}}\right)\right] + \left[e_g (A - A_{atm})\right] + \left[\lambda A z_{wc}\right]}{A_{gw}} \quad (8)$$

Atmospheric evasion is usually quantified using local wind speed measurements applied to theoretical gas exchange models (e.g., Macintyre et al., 1995). These equations appear to work reasonable well, at least under "normal" conditions, i.e., when the turbulence involved is derived from wind interactions, not from breaking waves or some other disturbance. Direct measurements of radon inventory losses in a protected boat basin in Sicily compared very well to those calculated from the gas exchange equations (Burnett and Dulaiova, 2006). Experimental estimates of ^{222}Rn exchange with the atmosphere can also be made by evaluating the respective slopes of ^{222}Rn and ^{224}Ra in surface waters away from a common source of these radioisotopes. This works because ^{222}Rn and ^{224}Ra have very similar half-lives and are affected in the same manner by mixing processes but only radon will emanate to the atmosphere. The common source

could be SGD, river input, a hot spot of natural radioactive minerals or any localized enrichment of ^{222}Rn and ^{224}Ra. Dulaiova and Burnett (2006) estimated the radon loss from surface waters in the Gulf of Thailand from the difference in the slopes of the ^{222}Rn and ^{224}Ra horizontal distributions across the inner shelf away from the mouth of the Chao Phraya River (Fig. 8). The estimated gas exchange velocities (k) based on their experimental results agreed well with theoretical models developed for lakes, estuaries and coastal systems.

Ellins et al. (1990), based on studies of streams in Puerto Rico was one of the first to show that ^{222}Rn measurements could be used to trace groundwater discharges into surface waters. Cable et al. (1996a), a few years later, provided the first example on the use of ^{222}Rn to quantify SGD to the coastal zone. These authors, working in the northeastern Gulf of Mexico, used a four box sub-pycnocline model (which was essentially the flux-by-difference approach) to derive SGD. The strong pycnocline that develops in the summer allowed the authors to look at fluid flow from the sediments into the bottom boundary layer without having to correct for the air-sea loss of ^{222}Rn. Cable et al. (1996b) also investigated SGD near a submarine spring in the same study region. In a transect across the spring outflow, they observed a ^{222}Rn increase of 10-50 fold over background activities. In addition, they found a strong correlation between seepage rate (as measured by seepage meters along shore-normal transects) and ^{222}Rn and CH_4 inventories in the water column along a nearby shoreline. In Chesapeake Bay, Hussain et al. (1999) observed an inverse ^{222}Rn variation with salinity, which they attributed to discharge of lower salinity groundwater near the head of the bay. Using a box model approach, they estimated that ^{222}Rn-derived SGD rates to Chesapeake Bay were on the order of 10% of the riverine flux of freshwater to the bay.

Schwartz (2003) identified a high SGD zone in the Delaware River and Bay Estuary based on the distribution of radon. Water column ^{222}Rn activity in this zone was significantly elevated relative to adjacent areas. Using a mass balance approach, it was shown that simple molecular diffusion from sediments could not support the observed excess radon and that a significant groundwater flux was required to account for the measured activity. The calculated SGD flux is equivalent to the surface water discharge of the second and third largest tributary rivers of the Delaware Estuary.

Garrison et al. (2003) used ^{222}Rn, as well as Si, Cl, and total alkalinity as natural tracers to measure SGD in Kahana Bay, Hawaii. Nutrient concentrations were also measured to calculate total nutrient fluxes into the bay via SGD. These authors determined that SGD provides a significant source of dissolved nutrients to the bay, and that terrestrial SGD was an important contributor to that nutrient supply. The ratio of SGD-derived to river-derived nutrient fluxes for total dissolved phosphorus and nitrogen were estimated to be 5:1 and 2:1, respectively.

Based on the measured mean inventory of ^{222}Rn in Eckernforder Bay, Baltic Sea (Germany), Purkl and Eisenhauser (2004) estimated the groundwater discharge rate using a 2-box model. The deduced SGD was in good agreement with that derived based on a numerical model. The inventories of ^{223}Ra and ^{224}Ra produced much higher apparent flow rates, perhaps because the applied endmember radium activities were based on fresh groundwater.

Hwang et al. (2005b) estimated SGD using a variety of tracers including ^{222}Rn and radium isotopes into Bangdu Bay, a semi-enclosed embayment on the Korean volcanic island, Jeju. Their estimated SGD rates were much higher than those reported from typical continental margins. The nutrient fluxes from SGD were about 90%, 20%, and 80% of the total input (excluding inputs from open ocean water) for dissolved inorganic nitrogen, phosphorus, and silica, respectively. The authors concluded that these excess nutrient inputs from SGD are the major sources of ‘‘new nutrients’’ to this bay and could contribute to eutrophication.

SGD was quantified by a variety of methods including ^{222}Rn for a 4-day period during the early summer of 2004, in Salt Pond on Cape Cod, USA (Crusius et al., 2005). Their results suggested that less than one quarter of the discharge occurred within the pond itself, while the remainder discharged immediately seaward of the pond. A box model achieved a reasonable fit to both the salinity and radon data assuming that the SGD was fresh and derived from outside the pond.

4.2 Applications to short (tidal) time scale variation in SGD

Historically, measurements of radon concentrations in the water column have been accomplished by standard oceanographic sampling and analysis techniques (radon emanation)

with special care required for trace gas sampling (Broecker, 1965; Mathieu et al., 1988). Recently, automated systems have become available, which may be applied to increase the sampling resolution and efficiency of the process. Burnett et al. (2001) demonstrated that a "continuous" radon monitor could provide reasonably high-resolution data on the radon concentration of coastal seawater at one location over time.

An automated radon system based on a commercial radon-in-air analyzer (RAD7, Durridge Corp.) analyzes ^{222}Rn from a constant stream of water (driven by a submersible pump) passing through an air-water exchanger that distributes radon from a running flow of water to a closed air loop. The air stream is fed to a radon monitor that determines the concentration of ^{222}Rn by collection and measurement of the α-emitting daughters, ^{214}Po and ^{218}Po. Since the distribution of radon at equilibrium between the air and water phases is governed by a well-known temperature dependence, the radon concentration in the water is easily calculated. A key advantage to this method is that changes in the inventory of ^{222}Rn over time, minus allowances for losses due to atmospheric evasion and mixing with lower concentration waters offshore, can be converted to fluxes (using a non-steady state derivation of equation 1, Burnett and Dulaiova, 2003).

Burnett et al. (2002), Lambert and Burnett (2003), and Burnett and Dulaiova (2003) made continuous ^{222}Rn measurements during multi-day deployments in Apalachee Bay (Northwest Florida, USA). Calculated radon fluxes were clearly not in steady state but fluctuated with an apparent period of approximately 12 hours, most likely a reflection of the mixed, semi-diurnal tides in this region. This periodicity on tidal time scales associated with SGD had been observed earlier from automated seepage meters (Paulsen et al., 2001; Taniguchi, 2002; Sholkovitz et al., 2003). This pattern is due to: (1) lower hydrostatic pressure at low tides causing increased seepage and thus higher radon fluxes; (2) a change in the hydraulic gradient in response to the tidal fluctuation; (3) recirculated seawater is moving through the shallow aquifer and sediments in response to tidal pumping; or (4) a combination of these processes.

Recent investigations have reported longer-term (weeks to months) tidally modulated cycles in seepage based on continuous measurements of the groundwater tracers radon and methane (Kim and Hwang, 2002) and automated seepage meter observations (Taniguchi, 2002). Both the tracer and seepage meter studies showed that there is not only a semi-diurnal or diurnal tidal relationship to SGD but also a semi-monthly variation in flow reflecting the neap-spring lunar cycle. Superimposed on this predictable behavior in tidally driven response are variations in terrestrial hydrologic parameters (water table height, etc.). This appeared in the ^{222}Rn and CH_4 tracer data from southern Korea, where Kim and Hwang (2002) noted that groundwater discharge was more limited in the dry season when the aquifer was not recharging. These results demonstrate the overlapping nature between terrestrial and marine SGD forcing components.

An SGD assessment intercomparison experiment was conducted in May, 2002, in West Neck Bay, located in the southwestern portion of Shelter Island (Long Island, New York). This intercomparison was one of several sponsored by the Scientific Committee on Oceanic Research (SCOR) and the Land-Ocean Interaction in the Coastal Zone (LOICZ) Project (Burnett et al., 2006). During these intercomparisons, several methods (isotopes, different types of seepage meters, etc.) were run side-by-side to evaluate their relative strengths and weaknesses. Figure 9 displays a comparison from the Shelter Island experiment of calculated radon fluxes (based on measurements from a continuous radon monitor) with seepage rates measured directly via a dye-dilution seepage meter. During the period (May 17-20) when both devices were operating at the same time, there is a clear and reproducible pattern of higher radon and water fluxes during the low tides. There is also a suggestion that the seepage spikes slightly led the radon fluxes, which is consistent with the notion that the groundwater seepage is the source of the radon. The results show excellent agreement in the range of advection rates determined and their average by these two completely independent methods.

4.3 Applications to mapping Rn distribution in the coastal ocean

One of the benefits of a continuous radon measurement system is that one can conduct surveys to locate where groundwater discharges may be more prevalent. The survey-mode system is based on a parallel arrangement of several (up to six have been used thus far) RAD7 radon-in-air monitors coupled to one exchanger. Integrated depth sounding, GPS navigation,

and temperature-conductivity measurements are usually included (Dulaiova et al., 2005). The water is pumped from a submersible pump near the water surface to an air-water exchanger and the air is directed to all detectors for measurement. With the increased sensitivity that the multiple detectors provide, one can shorten the measurement integration time to allow better spatial resolution. Response times on the order of 5-15 minutes are typical.

Stieglitz (2005) used a 2-detector system to measure ^{222}Rn activity along a ~250 km long shore-parallel transect about 1 km off the Great Barrier Reef (Australia) in April 2003. This survey showed localized radon elevations along parts of the coastline with two statistically significant peaks. These peaks were thought to be related to areas of known or suspected highs in SGD. These results suggest that continuous sampling of ^{222}Rn along a coastal transect is a useful, non-quantitative tool to reveal input zones of groundwater along a coastline on scales of hundreds of kilometers.

During another SGD assessment intercomparison in Ubatuba, Brazil (November 2003), the spatial distribution of radon in the surface waters along the shorelines of two embayments was assessed using a multi-detector radon system (Burnett et al., 2006b). The results showed that there were definite areas of higher radon in the two embayments investigated (Fig. 10). Small springs were observed in this area that consistently showed up as positive radon anomalies with lower salinities. Similar results were observed in a Rhode Island (USA) embayment, where Charette et al. (unpub. data) observed an inverse correlation between ^{222}Rn and salinity in the northeastern and northwestern embayments, indicating a major source of fresh SGD to the system (Fig. 11). In the southeastern portion of the pond, low salinity coupled with low radon indicates that the freshening was due almost entirely to surface water runoff.

4.4 Processes controlling endmember ^{222}Rn

A key issue when comparing techniques for measurement of SGD is the fluid composition that each method is measuring. Whereas hydrogeological techniques are estimates of fresh water component of SGD, the radium and radon methods also include a component of recirculated seawater. Unlike radium, ^{222}Rn is inert and salinity does not control its activity in groundwater. For all but the shallowest portions of the subterranean estuary, groundwater age is not expected

to exert a major control on ^{222}Rn distributions, as any groundwater with a subsurface residence time longer than a few weeks will have reached steady state in ^{222}Rn with the host sediment ^{226}Ra activity. Despite this, groundwater ^{222}Rn activities are often quite heterogeneous at a given study site. In a groundwater transect from Waquoit Bay, MA, ^{222}Rn (like ^{226}Ra) increased with increasing salinity, though ^{222}Rn was more than two orders of magnitude enriched in groundwater relative to average surface water at all salinities (Abraham et al., 2003). The source of higher activities in the saline zone is unclear, one possible source is a higher sediment ^{226}Ra concentration in offshore sediments (Abraham et al., 2003; Mulligan and Charette, 2006), resulting from the accumulation of Mn hydr(oxides) that scavenge radium (Charette et al., 2005). Variations in groundwater ^{222}Rn activities may also be a consequence of changing water-rock ratios in the subsurface. In a recent review of the importance of SGD to nutrient budgets, Kim and Swarzenski (2006) stated that "…in order to use Rn as a better SGD tracer, we have to improve techniques for measuring air-water exchange and for measuring Rn endmember values in groundwater that accurately represent the actual seeping submarine groundwater of the study region." We agree with this assessment and recommend that future research be directed in these areas.

5. Uranium

5.1 Impact of SGD on uranium cycling in the coastal ocean

More recently, the geochemical budget for uranium has been shown to be impacted by SGD. The approach to evaluate the impact of SGD on uranium cycling is based on the fact that uranium is generally enriched in seawater relative to fresh (low ionic strength) groundwater, and on two central assumptions. First, uranium must be carried by seawater into the sediments from regions of SGD during seawater circulation (Fig. 1). Second, the sediments must be reducing and the seawater must remain in contact with reducing sediments long enough to reduce the U^{6+} to U^{4+}. Uranium is typically conservative in oxic seawater where its oxidation state is +6 and it forms a strong complex with the carbonate ion (Koide and Goldberg, 1963). Under reducing conditions such as in organic-rich sediments or oxygen-poor groundwater, U(VI) is reduced to U(IV). In the +4 oxidation state, U is particle reactive and sorbs to the sediments making this reducing environments a sink for U (Cowart, 1980; Cochran et al., 1986). U(VI) can also be

removed from solution to solid phases in the presence of Fe (hydr)oxides, for which U(VI) has a relatively strong affinity, especially in freshwater.

Charette and Sholkovitz (2006) reported that the Waquoit Bay (Massachusetts, USA) subterranean estuary was a sink for uranium; U-salinity distribution displayed strong evidence of removal at intermediate salinity (Fig. 12a). In studies of coastal aquifers in Brazil and South Carolina, respectively, Windom and Niencheski (2003) and Duncan and Shaw (2003) observed significant U depletion at intermediate salinities, which they also attributed to removal under anoxic conditions. Such large-scale U removal observed in the subterranean estuary was also reflected in the U-salinity distribution of the surface water of Waquoit Bay (Fig. 12b), which yielded an average removal efficiency of about 50% for U. Based on these data and using a global SGD estimate of 4,000 km^3 y^{-1} (Burnett et al., 2003), it is estimated that SGD could annually remove ~ 20 x 10^6 mol U from the ocean. Such a removal flux would put SGD on par with the global U sink for marine sediments and salt marshes (both ~27 x 10^6 mol U y^{-1}see also Mckee this volume, Cochran and Kadko this volume), though the salt marsh estimate (Windom et al., 2000), likely includes the effects of SGD (Sibley, 2004).

5.2 Uranium as a potential new tracer of SGD

Because uranium is enriched in sea water relative to most coastal groundwater, the observed depletion of uranium in estuarine and coastal waters may provide an estimate of the sea water component of SGD that recharges coastal aquifers, or submarine groundwater recharge (SGR). If the redox conditions in the aquifer are adequate to convert U (VI) to U(IV) so that it is sequestered in the permeable sediments, deviations from conservative mixing in surface waters may be used to determine the fraction of U removed by SGR. This is expressed as the simple relationship:

$$\left(1-\frac{[\mathrm{U}]_{measured}}{[\mathrm{U}]_{predicted}}\right)\mathrm{x}100\% \qquad (9)$$

where $[U]_{measured}$ is U concentration (moles/kg), $[U]_{predicted}$ is U concentration predicted from the salinity assuming conservative mixing with the seawater endmember (moles/kg). If we assume that all of the U is removed during SGR and that this is the only process affecting nonconservative behavior of U, the fraction of U depletion in the water column is the fraction of the tidal prism that circulates through the subterranean estuary. If the residence time of the surface water can be determined by other means, the fraction of the tidal prism can be converted to the flux of SGR. If not all of the U is removed during passage through the subterranean estuary, SGR will be larger than estimated.

Moore and Shaw (submitted) used the salinity-normalized U deficit in the surface water of several southeastern U.S. estuaries to estimate that 15-50 % of the tidal prism volume is exposed to conditions reducing enough to deplete U in these systems. Because such conditions occur almost exclusively in sediment pore waters, they assumed any U deficit was a proxy for flow through permeable sediments, i.e. no other processes removed U. The fraction of the tidal prism based on U removal reflects only recirculation as a component of SGD; it does not estimate meteoric water discharge. This approach assumes that removal under reducing conditions dominates in the high salinity section of the salt marsh. By evaluating U removal from the tidal prism in the low marsh, this estimate does not include U removal that may occur under oxic conditions in the high marsh water column (as observed by Church et al., 1996).

6. Synthesis of existing studies

The study of SGD by marine and environmental scientists is advancing at a rapid pace. A number of these studies have directly compared fluxes derived from Ra and Rn (Fig. 13; Table 1). These include a series of SGD intercomparison experiments (Burnett et al., 2002; Burnett et al., 2003; Burnett et al., 2006a) and individual studies (e.g., Hwang et al., 2005a; Mulligan and Charette, 2006). In general, the agreement between the two techniques has been good, considering their different geochemical behavior and source/sink terms (other than SGD). Where differences exist, they can often be explained by differences in measurement scale. The ^{222}Rn signature of SGD is best observed near the source, due to its short half-life. In contrast, ^{226}Ra has the ability to integrate the SGD signal over much wider spatial scales. Lastly, of the intercomparison studies conducted to date, there appears to be no systematic difference in the

two techniques based on the coastal hydrogeologic setting, though a wider range of estimates was typically observed in areas with fractured crystalline rock aquifers and where springs were a major conduit for SGD (Burnett et al., 2006a).

Given the influence of salinity on radium and its isotopes (but not on ^{222}Rn), it stands to reason that the two techniques may not always return the same SGD estimate (see section 2.4). This seems to occur when fresh groundwater input is substantial relative to recirculated seawater component of SGD (Mulligan and Charette, 2006; Charette, 2007). It may also be related to the scale of the study area; utilizing the flux-by-difference approach for a small "box" near the zone of fresh discharge may inherently exclude a large amount of recirculated seawater. This issue is discussed further in section 7.

Failure to understand that SGD often includes a substantial component of seawater that has been recirculated through and reacted with coastal marine sediments has led to some controversy and confusion in the literature. These problems are usually due to the observation that Darcy's Law and other traditional hydrogeologic-based groundwater flux estimates are often significantly lower than SGD measured by radionuclide models and seepage meters (Younger, 1996; Burnett et al., 2001; Smith and Zawadzki, 2003). Using a model that included the terrestrial hydraulic gradient and density-dependent flow, Smith and Zawadzki (2003) were only able to explain 10% of the SGD measured by seepage meters and radium and radon box models. They concluded that fluid circulation and discharge, which were not explicitly included in their model, were responding to variations in fluid pressure generated in the marine water column.

7. Towards a global estimate of SGD

At present, there are no global estimates of SGD that are based on any U-Th series nuclides. Zekster (2000) estimated total global fresh SGD at 2,400 $km^3\ y^{-1}$, or 11 $m^3\ m^{-1}\ d^{-1}$ when normalized to the total global coastline length (Table 1). Shore line normalized units allow for site to site comparisons of SGD regardless of the scale of the study area. Riedl et al. (1972) estimated the intertidal pump to be approximately half the global fresh SGD (5.34 $m^3\ m^{-1}\ d^{-1}$) and the subtidal pump at nearly 40 times that value (437 $m^3\ m^{-1}\ d^{-1}$), the latter of which highlights the importance of seawater circulation through coastal marine sediments in coastal

geochemical budgets. Curiously, the median value among the local scale studies (12 m^3 m^{-1} d^{-1}) is of the same order of magnitude as the Zekster (2000) terrestrial and Riedl et al. (1972) intertidal groundwater fluxes. In contrast, the regional studies were on average significantly higher and similar to the Riedl et al. (1972) subtidal pump flux. Two exceptions to this difference are the Pettaquamscutt Estuary (42-420 m^3 m^{-1} d^{-1}) and the Chao Phraya estuary (200 m^3 m^{-1} d^{-1}), which is likely due to the fact that they are the only river-type estuaries represented in this compilation; their shoreline geometry is such that it tends to focus SGD away from the coastline and into the river itself.

The observation that the shoreline normal fluxes tend to correlate with the scale of the study is particularly unusual given that in many cases they were conducted in the same region or had similar coastal geology. It is also unusual in that local-scale studies have tended to specifically target areas of known SGD (and therefore usually enhanced), which one might assume would result in higher fluxes on average. One likely explanation for the difference is that the larger scale studies are capturing the subtidal pump, which would be significantly more important on the scale of the continental shelf, whereas the smaller scale studies are only measuring the terrestrial and intertidal contributions to SGD. Additionally, the small scale studies have been conducted during relatively calm conditions; the large-scale studies may capture effects of storms (Moore and Wilson, 2005).

An accurate estimate of global SGD based on U-Th series tracers will require a more refined approach. One possibility would involve the use of coastal groundwater typology (Bokuniewicz, 2001; Bokuniewicz et al., 2003). The typology approach involves applying a subset of SGD-relevant parameters (e.g., rainfall, evapotranspiration, topography) from the Land-Ocean Interaction in the Coastal Zone (LOICZ) database (Maxwell and Buddemeier, 2002; http://www.palantir.swarthmore.edu/loicz/) to estimate the relative importance of SGD along a model of the global coastline. Such a model could be calibrated with existing local or regional scale U-Th series studies as highlighted in Table 1. One advantage of such an approach would be that the SGD associated with each coastal hydrogeologic setting (e.g., coastal plain, karst, volcanic) would be appropriately weighted.

8. Perspective and Future Directions

One of the main advantages of the use of the natural geochemical tracer approach to assessment of SGD is that the water column tends to integrate the signal. As a result, smaller-scale variations, which may be unimportant for larger-scale studies, are smoothed out. The approach may thus be optimal in environments where especially large spatial variation is expected (e.g., fractured rock aquifers). In addition to the spatial integration, tracers integrate the water flux over the time-scale of the isotope and the water residence time of the study area. Depending upon what one wants to know, this can often be a great advantage. Mixing and atmospheric exchanges (radon) must be evaluated as described earlier and care must be exercised in defining the end-members. The use of multiple tracers (e.g., both radon and radium isotopes) is recommended when possible.

Evaluation of larger-scale systems via U/Th isotopes will become more practical as the technology and our understanding of these systems improves. Indeed, a global estimate of SGD via U/Th nuclides should soon be within our reach. This should provide an interesting and useful constraint on other independent assessments of this flow.

Acknowledgments

This chapter was greatly improved by the comments from the editors and Aaron Beck. The authors acknowledge support from the U.S. National Science Foundation (OCE04-25061, MAC; OCE02-33657, WSM; OCE05-20723, WCB).

References

Abraham, D. M., M. A. Charette, M. C. Allen, A. Rago, and K. D. Kroeger. (2003). Radiochemical estimates of submarine groundwater discharge to Waquoit Bay, Massachusetts. *Biological Bulletin* **205:** 246-247.

Boehm, A. B., A. Paytan, G. G. Shellenbarger, and K. A. Davis. (2006). Composition and flux of groundwater from a California beach aquifer: Implications for nutrient supply to the surf zone. *Continental Shelf Research* **26:** 269-282.

Boehm, A. B., G. G. Shellenbarger, and A. Paytan. (2004). Groundwater discharge: Potential association with fecal indicator bacteria in the surf zone. *Environmental Science & Technology* **38:** 3558-3566.

Bokuniewicz, H. (2001). Toward a coastal ground-water typology. Journal of Sea Research **46:** 99-108.

Bokuniewicz, H., R. Buddemeier, B. Maxwell, and C. Smith. (2003). The typological approach to submarine groundwater discharge. *Biogeochemistry* **66:** 145-148.

Bollinger, M. S., and W. S. Moore. (1993). Evaluation of salt marsh hydrology using radium as a tracer. *Geochimica et Cosmochimica Acta* **57:** 2203-2212.

Breier, J. A., C. F. Breier, and H. N. Edmonds. (2005). Detecting submarine groundwater discharge with synoptic surveys of sediment resistivity, radium, and salinity. *Geophysical Research Letters* **32:** doi: 10.1029/2005GL 024639.

Broecker, W. S. (1965). An application of natural radon to problems in ocean circulation, In: Symposium on diffusion in oceans and fresh waters. (Ed. T. Ichite), Lamont-Doherty Geological Observatory, New York, pp 116-145.

Burnett, W. C., J. B. Cowart, and S. Deetae. (1990). Radium in the Suwannee River and Estuary: Spring and River Input to the Gulf of Mexico. *Biogeochemistry* **10:** 237-255.

Burnett, W. C., H. Bokuniewicz, M. Huettel, W. S. Moore, and M. Taniguchi, (2003). Groundwater and pore water inputs to the coastal zone, *Biogeochemistry* **66**, 3-33.

Burnett, W. C., P. K. Aggarwal, A. Aureli, H. Bokuniewicz, J. E. Cable, M. A. Charette, E. Kontar, S. Krupa, K. M. Kulkarni, A. Loveless, W. S. Moore, J. A. Oberdorfer, J. Oliveira, N. Ozyurt, P. Povinec, A. M. G. Privitera, R. Rajar, R. T. Ramessur, J. Scholten, T. Stieglitz, M. Taniguchi, and J. V. Turner. (2006). Quantifying submarine groundwater discharge in the coastal zone via multiple methods. *Science of the Total Environment* **367:** 498-543.

Burnett, W. C. (2002). Assessing methodologies for measuring groundwater discharge to the ocean.

EOS **83:** 117-123.

Burnett, W. C., and H. Dulaiova. (2003). Estimating the dynamics of groundwater input into the coastal zone via continuous radon-222 measurements. *Journal of Environmental Radioactivity* **69:** 21-35.

Burnett, W. C. and H. Dulaiva. (2006). Radon as a tracer of submarine groundwater discharge into a boat basin in Donnalucata, Sicily. *Continental Shelf Research* **26:** 862-873.

Burnett, W. C., G. Kim, and D. Lane-Smith. (2001). A continuous monitor for assessment of Rn-222 in the coastal ocean. *Journal of Radioanalytical and Nuclear Chemistry* **249:** 167-172.

Burnett, W. C., G. Wattayakorn, M. Taniguchi, H. Dulaiova, P. Sojisuporn, S. Rungsupa, and T. Ishitobi. (2007). Groundwater-derived nutrient inputs to the Upper Gulf of Thailand. *Continental Shelf Research* **27**: 176-190.

Cable, J. E., W. C. Burnett, and J. P. Chanton. (1997). Magnitude and variations of groundwater seepage along a Florida marine shoreline. *Biogeochemistry* **38:** 189-205.

Cable, J. E., G. C. Bugna, W. C. Burnett, and J. P. Chanton. (1996). Application of Rn-222 and CH_4 for assessment of groundwater discharge to the coastal ocean. *Limnology and Oceanography* **41:** 1347-1353.

Cable, J. E., W. C. Burnett, J. P. Chanton, and G. L. Weatherly. (1996). Estimating groundwater discharge into the northeastern Gulf of Mexico using radon-222. *Earth and Planetary Science Letters* **144:** 591-604.

Capone, D. G., and M. F. Bautista. (1985). A groundwater source of nitrate in nearshore marine sediments. *Nature* **313:** 214-216.

Capone, D. G., and J. M. Slater. (1990). Interannual Patterns of Water-Table Height and Groundwater Derived Nitrate in Nearshore Sediments. *Biogeochemistry* **10:** 277-288.

Charette, M. A. (2007). Hydrologic forcing of submarine groundwater discharge: insight from a seasonal study of radium isotopes in a groundwater dominated salt marsh estuary. *Limnology and Oceanography* **52:** 230-239.

Charette, M. A., and K. O. Buesseler. (2004). Submarine groundwater discharge of nutrients and copper to an urban subestuary of Chesapeake bay (Elizabeth River). *Limnology and Oceanography* **49:** 376-385.

Charette, M.A., and M.C. Allen. (2006). Precision groundwater sampling in coastal aquifers using a direct push shielded-screen well-point system. *Ground Water Monitoring & Remediation* **26**, 87-93.

Charette, M. A., K. O. Buesseler, and J. E. Andrews. (2001). Utility of radium isotopes for evaluating the input and transport of groundwater-derived nitrogen to a Cape Cod estuary. *Limnology and Oceanography* **46:** 465-470.

Charette, M. A., and E. R. Sholkovitz. (2002). Oxidative precipitation of groundwater-derived ferrous iron in the subterranean estuary of a coastal bay. *Geophysical Research Letters* **29:** doi: 10.1029/2001GL 014512.

Charette, M. A., and E. R. Sholkovitz. (2006). Trace element cycling in a subterranean estuary: Part 2. Geochemistry of the pore water. *Geochimica et Cosmochimica Acta* **70:** 811-826.

Charette, M. A., E. R. Sholkovitz, and C. M. Hansel. (2005). Trace element cycling in a subterranean estuary: Part 1. Geochemistry of the permeable sediments. *Geochimica et Cosmochimica Acta* **69:** 2095-2109.

Charette, M. A., R. Splivallo, C. Herbold, M. S. Bollinger, and W. S. Moore. (2003). Salt marsh submarine groundwater discharge as traced by radium isotopes. *Marine Chemistry* **84:** 113-121.

Church, T. M., M. M. Sarin, M. Q. Fleisher, and T. G. Ferdelman. (1996). Salt marshes: An important coastal sink for dissolved uranium. *Geochimica et Cosmochimica Acta* **60:** 3879-3887.

Cochran, J. K., A. E. Carey, E. Sholkovitz and D. Surprenant. (1986). The geochemistry of uranium and thorium in coastal marine sediments and sediment pore waters. *Geochimica et Cosmochimica Acta* **50:** 663-680.

Cooper, H. H., Jr. (1959). A hypothesis concerning the dynamic balance of fresh water and salt water in a coastal aquifer. *Journal of Geophysical Research-Oceans* **64:** 461-467.

Corbett, D. R., W. C. Burnett, P. H. Cable, and S. B. Clark. (1997). Radon tracing of groundwater input to Par Pond, Savannah River site. *Journal of Hydrology* **203:** 209-227.

Corbett, D. R., J. Chanton, W. Burnett, K. Dillon, C. Rutkowski, and J. W. Fourqurean. (1999). Patterns of groundwater discharge into Florida Bay. *Limnology and Oceanography* **44:** 1045-1055.

Corbett, D. R., K. Dillon, W. Burnett, and J. Chanton. (2000). Estimating the groundwater contribution into Florida Bay via natural tracers, Rn-222 and CH_4. *Limnology and Oceanography* **45:** 1546-1557.

Cowart, J. B. (1980). The relationship of uranium isotopes to oxidation-reduction in the Edwards

carbonate aquifer of Texas. *Earth and Planetary Science Letters* **48:** 277-283.

Crotwell, A. M., and W. S. Moore. (2003). Nutrient and radium fluxes from submarine groundwater discharge to Port Royal Sound, South Carolina. *Aquatic Geochemistry* **9:** 191-208.

Crusius, J., D. Koopmans, J. F. Bratton, M. A. Charette, K. Kroeger, P. Henderson, L. Ryckman, K. Halloran, and J. A. Colman. (2005). Submarine groundwater discharge to a small estuary estimated from radon and salinity measurements and a box model. *Biogeosciences* **2:** 141-157.

D'elia, C. F., K. L. Webb, and J. W. Porter. (1981). Nitrate-rich groundwater inputs to Discovery Bay, Jamaica: A significant source of N to local coral reefs? *Bulletin of Marine Science* **31:** 903-910.

Destouni, G., and C. Prieto. (2003). On the possibility for generic modeling of submarine groundwater discharge. *Biogeochemistry* **66:** 171-186.

Dulaiova, H., and W. C. Burnett. (2006). Radon loss across the water-air interface (Gulf of Thailand) estimated experimentally from Rn-222-Ra-224. *Geophysical Research Letters* **33:** doi:10.1029/2005GL025023.

Dulaiova, H., W. C. Burnett, J. P. Chanton, W. S. Moore, H. J. Bokuniewicz, M. A. Charette, and E. Sholkovitz. (2006). Assessment of groundwater discharges into West Neck Bay, New York, via natural tracers. *Continental Shelf Research* **26:** 1971-1983.

Dulaiova, H., W. C. Burnett, G. Wattayakorn, and P. Sojisuporn. (2006). Are groundwater inputs into river-dominated areas important? The Chao Phraya River – Gulf of Thailand. *Limnology and Oceanography* **51:** 2232-2247.

Dulaiova, H., R. Peterson, W. C. Burnett, and D. Lane-Smith. (2005). A multi-detector continuous monitor for assessment of Rn-222 in the coastal ocean. *Journal of Radioanalytical and Nuclear Chemistry* **263:** 361-365.

Duncan, T., and T. J. Shaw. (2003). The mobility of rare earth elements and redox sensitive elements in the groundwater/seawater mixing zone of a shallow coastal aquifer. *Aquatic Geochemistry* **9:** 233-255.

Ellins, K. K., A. Romanmas, and R. Lee. (1990). Using Rn-222 to Examine Groundwater Surface Discharge Interaction in the Rio-Grande-De-Manati, Puerto-Rico. *Journal of Hydrology* **115:** 319-341.

Garrison, G. H., C. R. Glenn, and G. M. McMurtry. (2003). Measurement of submarine groundwater discharge in Kahana Bay, O'ahu, Hawai'i *Limnology and Oceanography* **48:** 920-928.

Hancock, G. J., and A. S. Murray. (1996). Source and distribution of dissolved radium in the Bega River

estuary, Southeastern Australia. *Earth and Planetary Science Letters* **138:** 145-155.

Hussain, N., T. M. Church, and G. Kim. (1999). Use of ^{222}Rn and ^{226}Ra to trace groundwater discharge into the Chesapeake Bay. *Marine Chemistry* **65:** 127-134.

Hwang, D. W., G. B. Kim, Y. W. Lee, and H. S. Yang. (2005a). Estimating submarine inputs of groundwater and nutrients to a coastal bay using radium isotopes. *Marine Chemistry* **96:** 61-71.

Hwang, D. W., Y. W. Lee, and G. Kim. (2005b). Large submarine groundwater discharge and benthic eutrophication in Bangdu Bay on volcanic Jeju Island, Korea. *Limnology and Oceanography* **50:** 1393-1403.

Johannes, R. E. (1980). The ecological significance of submarine discharge of groundwater. *Marine Ecology Progress Series*. **3:** 365-373.

Kelly, R. P., and S. B. Moran. (2002). Seasonal changes in groundwater input to a well-mixed estuary estimated using radium isotopes and implications for coastal nutrient budgets. *Limnology and Oceanograph*y **47:** 1796-1807.

Kim, G., and D. W. Hwang. (2002). Tidal pumping of groundwater into the coastal ocean revealed from submarine Rn-222 and CH_4 monitoring. *Geophysical Research Letters* **29:** doi: 10.1029/2002GL015093.

Kim, G., K. K. Lee, K. S. Park, D. W. Hwang, and H. S. Yang. (2003). Large submarine groundwater discharge (SGD) from a volcanic island. *Geophysical Research Letters* **30:** doi: 10.1029/GRL018378.

Kim, G., J. W. Ryu, H. S. Yang, and S. T. Yun. (2005). Submarine groundwater discharge (SGD) into the Yellow Sea revealed by Ra-228 and Ra-226 isotopes: Implications for global silicate fluxes. *Earth and Planetary Science Letters* **237:** 156-166.

Kim, G., and P. W. Swarzenski. (2005). Submarine groundwater discharge (SGD) and associated nutrient fluxes to the coastal ocean. *In* Carbon and Nutrient Fluxes in Continental Margins: A Global Synthesis. Eds., K.-K. Liu, L. Atkinson, R. Quinones, and L. Talaue-McManus. Springer-Verlag, New York.

Koide, M., and E. D. Goldberg. (1963). Uranium-234/Uranium-238 ratios in sea water. *Progress in Oceanography* **3:** 173-177.

Krest, J. M., and J. W. Harvey. (2003). Using natural distributions of short-lived radium isotopes to quantify groundwater discharge and recharge. *Limnology and Oceanography* **48:** 290-298.

Krest, J. M., W. S. Moore, L. R. Gardner, and J. T. Morris. (2000). Marsh nutrient export supplied by

groundwater discharge: Evidence from radium measurements. *Global Biogeochemical Cycles* **14:** 167-176.

Krishnaswami, S., R. Bushan, and M. Baskaran. (1991). Radium isotopes and ^{222}Rn in shallow brines, Kharaghoda (India) *Chemical Geology* **87:** 125-136.

Lambert, M. J., and W. C. Burnett. (2003). Submarine groundwater discharge estimates at a Florida coastal site based on continuous radon measurements. *Biogeochemistry* **66:** 55-73.

Lapointe, B. E., J. D. O'connell, and G. S. Garrett. (1990). Nutrient coupling between on-site sewage disposal systems, groundwaters and nearshore surface waters of the Florida Keys. *Biogeochemistry* **10:** 289-307.

Laroche, J., R. Nuzzi, R. Waters, K. Wyman, P. G. Falkowski, and D. W. R. Wallace. (1997). Brown tide blooms in Long Island's coastal waters linked to interannual variability in groundwater flow. *Global Change Biology* **3:** 397-410.

Li, Y.-H., and L-H Chan. (1979). Desorption of Ba and ^{226}Ra from river-borne sediments in the Hudson Estuary. *Earth and Planetary Science Letters* **43:** 343-350.

Macintyre, S., R. H. Wanninkhof, and J. P. Chanton. (1995). Trace gas exchange across the air-water interface in freshwater and coastal marine environments, *In* Methods in ecology-biogenic trace gases: Measuring emissions from soil and water. Eds: P. A. Matson and R. C. Harris. Blackwell Science.

Mathieu, G. G., P. E. Biscaye, R. A. Lupton, and D. E. Hammond. (1988). System for measurement of ^{222}Rn at low levels in natural waters. *Health Physics* **55:** 989-992.

Maxwell, B., and R. Buddemeier. (2002). Coastal typology development with heterogeneous data sets. *Regional Environmental Change* **3:** 77-87.

Michael, H. A., A. E. Mulligan, and C. F. Harvey. (2005). Seasonal oscillations in water exchange between aquifers and the coastal ocean. *Nature* **436:** 1145-1148.

Monsen, N. E., J. E. Cloern, and L. V. Lucas. (2002). A comment on the use of flushing time, residence time, and age as transport time scales. *Limnology and Oceanography* **47:** 1545-1553.

Moore, W. S. (1987). Radium-228 in the South Atlantic Bight. *Journal of Geophysical Research-Oceans* **92:** 5177-5190.

Moore, W. S., H. Astwood, and C. Lindstrom. (1995). Radium isotopes in coastal waters on the Amazon shelf. *Geochimica et Cosmochimica Acta* **59:** 4285-4298.

Moore, W. S. (1996). Large groundwater inputs to coastal waters revealed by Ra-226 enrichments.

Nature **380:** 612-614.

Moore, W. S. (1997). High fluxes of radium and barium from the mouth of the Ganges-Brahmaputra river during low river discharge suggest a large groundwater source. *Earth and Planetary Science Letters* **150:** 141-150.

Moore, W. S. (1999). The subterranean estuary: a reaction zone of ground water and sea water. *Marine Chemistry* **65:** 111-125.

Moore, W. S. (2000). Determining coastal mixing rates using radium isotopes. *Continental Shelf Research* **20:** 1993-2007.

Moore, W. S. (2000). Ages of continental shelf waters determined from ^{223}Ra and ^{224}Ra. *Journal of Geophysical Research* **105:**22117-22122.

Moore, W. S. (2003). Sources and fluxes of submarine groundwater discharge delineated by radium isotopes. *Biogeochemistry* **66:** 75-93.

Moore, W. S. (2006). Radium isotopes as tracers of submarine groundwater discharge in Sicily. *Continental Shelf Research* **26:** 852-861.

Moore, W. S., J. O. Blanton, and S. Joye. (2006). Estimates of Flushing Times, Submarine Groundwater Discharge, and Nutrient Fluxes to Okatee River, South Carolina. *Journal of Geophysical Research-Oceans* **111:** doi: 10.1029/2005JC003041.

Moore, W. S., J. Krest, G. Taylor, E. Roggenstein, S. Joye, and R. Lee. (2002). Thermal evidence of water exchange through a coastal aquifer: Implications for nutrient fluxes. *Geophysical Research Letters* **29**: doi: 10.1029/2002GL014923.

Moore, W. S., and T. J. Shaw. (1998). Chemical signals from submarine fluid advection onto the continental shelf. *Journal of Geophysical Research-Oceans* **103:** 21543-21552.

Moore, W. S., and T. J. Shaw. (2006). Fluxes and behavior of radium isotopes, barium, and uranium in Southeastern US rivers and estuaries. *Marine Chemistry* Submitted.

Moore, W. S., and A. M. Wilson. (2005). Advective flow through the upper continental shelf driven by storms, buoyancy, and submarine groundwater discharge. *Earth and Planetary Science Letters* **235:** 564-576.

Mulligan, A. E., and M. A. Charette. (2006). Intercomparison of submarine groundwater discharge estimates from a sandy unconfined aquifer. *Journal of Hydrology* **327:** 411-425.

Nixon, S. W., C. A. Oviatt, J. Frithsen, and B. Sullivan. (1986). Nutrients and the productivity of estuarine and coastal marine ecosystems. *Journal Limnological Society*, *South Africa* **12:** 43-71.

Oberdorfer, J. A., M. A. Valentino, and S. V. Smith. (1990). Groundwater Contribution to the Nutrient Budget of Tomales Bay, California. *Biogeochemistry* **10:** 199-216.

Paulsen, R. J., C. F. Smith, D. O'Rourke, and T. F. Wong. (2001). Development and evaluation of an ultrasonic ground water seepage meter. *Ground Water* **39:** 904-911.

Paytan, A., G. S. Shellenbarger, K. Davis, J. H. Street, M. B. Young, and W. S. Moore. (2006). Submarine groundwater discharge: An important source of new inorganic nitrogen to coral reef ecosystems. *Limnology and Oceanography* **51:** 339-342.

Povinec, P. P., J. La Rosa, S.-H. Lee, S. Mulsow, I. Osvath, and E. Wyse. (2001). Recent developments in radiometric and mass spectrometry methods for marine radioactivity measurements. *Journal of Radioanalytical and Nuclear Chemistry* **248:** 713-718.

Purkl, S., and A. Eisenhauer. (2004). Determination of radium isotopes and Rn-222 in a groundwater affected coastal area of the Baltic Sea and the underlying sub-sea floor aquifer. *Marine Chemistry* **87:** 137-149.

Rama, and W. S. Moore. (1996). Using the radium quartet for evaluating groundwater input and water exchange in salt marshes. *Geochimica et Cosmochimica Acta* **60:** 4645-4652.

Riedl, R. J., N. Huang, and R. Machan. (1972). The subtidal pump: a mechanism of interstitial water exchange by wave action. *Marine Biology* **13:** 210-221.

Schwartz, M. C. (2003). Significant groundwater input to a coastal plain estuary: assessment from excess radon. *Estuarine Coastal and Shelf Science* **56:** 31-42.

Shaw T. J., W. S. Moore, J. Kloepfer, and M. Sochaski (1998). The flux of barium to the coastal waters of the southeastern USA: the importance of submarine groundwater discharge. *Geochimica et Cosmochimica Acta* **62**, 3047-3054.

Sholkovitz, E. R., C. Herbold, and M. A. Charette. (2003). An automated dye-dilution based seepage meter for the time-series measurement of submarine groundwater discharge. *Limnology and Oceanography*: Methods **1:** 17-29.

Sibley, S. D. (2004). The Impact of Salt Marsh Hydrogeology on Dissolved Uranium. M.S. thesis, Georgia Institute of Technology.

Simmons Jr., G. M. (1992). Importance of submarine groundwater discharge (SGWD) and seawater cycling to the material flux across sediment/water interfaces in marine environments. *Marine Ecology Progress Series* **84:** 173-184.

Smith, L., and W. Zawadzki. (2003). A hydrogeologic model of submarine groundwater discharge:

Florida intercomparison experiment. *Biogeochemistry* **66:** 95-110.

Stieglitz, T. (2005). Submarine groundwater discharge into the near-shore zone of the Great Barrier Reef, Australia. *Marine Pollution Bulletin* **51:** 51-59.

Swarzenski, P. W., C. D. Reich, R. M. Spechler, J. L. Kindinger, and W. S. Moore. (2001). Using multiple geochemical tracers to characterize the hydrogeology of the submarine spring off Crescent Beach, Florida. *Chemical Geology* **179:** 187-202.

Talbot, J. M., K. D. Kroeger, A. Rago, M. C. Allen, and M. A. Charette. (2003). Nitrogen flux and speciation through the subterranean estuary of Waquoit Bay, Massachusetts. *Biological Bulletin* **205:** 244-245.

Taniguchi, M. (2002). Tidal effects on submarine groundwater discharge into the ocean. *Geophysical Research Letters* **29:** doi**:** 10.1029/2002GL014987.

Valiela, I., J. L. Bowen, and K. D. Kroeger. (2002). Assessment of models for estimation of land-derived nitrogen loads to shallow estuaries. *Applied Geochemistry* **17:** 935-953.

Valiela, I., J. Costa, K. Foreman, J. M. Teal, B. Howes, and D. Aubrey. (1990). Transport of Groundwater-Borne Nutrients from Watersheds and Their Effects on Coastal Waters. *Biogeochemistry* **10:** 177-197.

Valiela, I., K. Foreman, M. LaMontagne, J. Costa, P. Peckol, B. DeMeo-Anderson, C. D'Avanzo, M. Babione, C. Sham, J. Brawley, and K. Lajtha. (1992). Couplings of Watersheds and Coastal Waters - Sources and Consequences of Nutrient Enrichment in Waquoit Bay, Massachusetts. *Estuaries* **15:** 443-457.

Valiela, I., J. M. Teal, S. Volkmann, D. Shafer, and E. J. Carpenter. (1978). Nutrient and particulate fluxes in a salt marsh ecosystem: tidal exchanges and inputs by precipitation and groundwater. *Limnology and Oceanography* **23:** 798-812.

Windom, H., and F. Niencheski. (2003). Biogeochemical processes in a freshwater-seawater mixing zone in permeable sediments along the coast of Southern Brazil. *Marine Chemistry* **83:** 121-130.

Windom, H., R. Smith, N. F., and A. C. (2000). Uranium in rivers and estuaries of globally diverse, smaller watersheds. *Marine Chemistry* **68:** 307-321.

Windom, H. L., W. S. Moore, L. F. H. Niencheski, and R. A. Jahnke. (2006). Submarine Groundwater Discharge: a Large, Previously Unrecognized Source of Dissolved Iron to the South Atlantic Ocean. *Marine Chemistry* **102:** 252-266.

Yang, H. S., D. W. Hwang, and G. B. Kim. (2002). Factors controlling excess radium in the Nakdong

River estuary, Korea: submarine groundwater discharge versus desorption from riverine particles. *Marine Chemistry* **78:** 1-8.

Younger, P.L., (1996). Submarine Groundwater Discharge. *Nature* **382**, 121-122.

Zektser, I. S. (2000). Groundwater and the Environment: Applications for the Global Community. Lewis Publishers. Boca Raton, 175 pp.

Figure Captions

Figure 1. Principal pathways for submarine groundwater discharge (SGD) to the coastal ocean. "Fresh", "Brackish" and "Saline" refer to the approximate salinity of the pore water. "Pore water" and "groundwater" are used interchangeably throughout this manuscript.

Figure 2. Generalized box model for using U-Th series isotopes as an index of fluid advection into coastal waters.

Figure 3. The distribution of ^{226}Ra offshore South Carolina. The results show high activities on the inner shelf that decrease offshore. Moore (1996) used the excess ^{226}Ra to estimate regional SGD fluxes.

Figure 4. Radium isotopes in samples from coastal northwest Florida. Near shore surface water samples (shown as squares) fall on a trend having a ^{228}Ra/^{226}Ra mixing ratio = 2.5. Most samples collected offshore (also shown as squares) fall on the same trend. Some samples collected offshore (circles) have lower salinity and fall below the trend for the other offshore samples. These lower salinity samples fall near a mixing line that includes samples collected near a submarine spring (open triangles) and an onshore artesian well from the Florida aquifer (triangles). The mixing ratio for these samples is 0.34. These data illustrate the use of the long-lived Ra isotopes for differentiating signals derived from the surficial and the Floridan aquifers. Adapted from Moore (2003).

Figure 5. One year, monthly time series of xs^{228}Ra and xs^{226}Ra (xs^{22x}Ra = ^{22x}Ra$_{estuary}$ – ^{22x}Ra$_{open\ ocean}$) in the Pettaquamscutt River, Rhode Island, USA illustrating the seasonal pattern in SGD. Adapted from Kelly and Moran (2002).

Figure 6. ^{226}Ra across a salinity gradient in the aquifer beneath the head of Waquoit Bay (Massachusetts, USA) during (a) March 2003 and (b) June 2003. The average bay water ^{226}Ra is also shown (salinity = 30).

Figure 7. Scatter diagram of the concentrations of total dissolved nitrogen and phosphorus with ^{226}Ra in samples from monitoring wells (excluding K) off the South Carolina, USA coast. The data show strong positive correlations. Adapted from Moore et al. (2002).

Figure 8. Scatter plots of radon and ^{224}Ra vs. radium ages along an offshore transect in the Upper Gulf of Thailand in January (A) and in July (B), 2004. The high inshore activities of ^{222}Rn and ^{224}Ra are due to SGD and release from particles for radium. Since the two nuclides have similar sources and half-lives, the radon air-water exchange rate can be estimated from the difference in the slopes of the ^{222}Rn and ^{224}Ra horizontal distributions.

Figure 9. Plot comparing variations in SGD at Shelter Island, New York between an automated seepage meter and the continuous radon method.

Figure 10. Distribution of ^{222}Rn in surface waters of Flamengo Bay (Ubatuba, Brazil) measured by a multi-detector radon mapping system. The heights of the bars correspond to the measured activities. Concentrations are in units of dpm/L.

Figure 11. Map of radon levels and salinity at Ninigret Pond, Rhode Island, USA on May 11, 2005 obtained using a multi-detector radon mapping system. High radon and low salinity is found in two embayments on the mainland side the pond, suggesting these are regions of enhanced discharge.

Figure 12. A comparison of groundwater and surface water concentrations of dissolved U at Waquoit Bay (Massachusetts, USA). (a) Groundwater U versus salinity for July 2002. Also shown is the bay water U collected during 1999. The dashed line indicates the conservative mixing line between the open ocean and fresh groundwater endmembers. (b) Expanded U-salinity distribution plot for the surface waters and the interpolated concentration of U at zero salinity.

Figure 13. Comparison of radium and radon derived SGD at various locations around the globe.

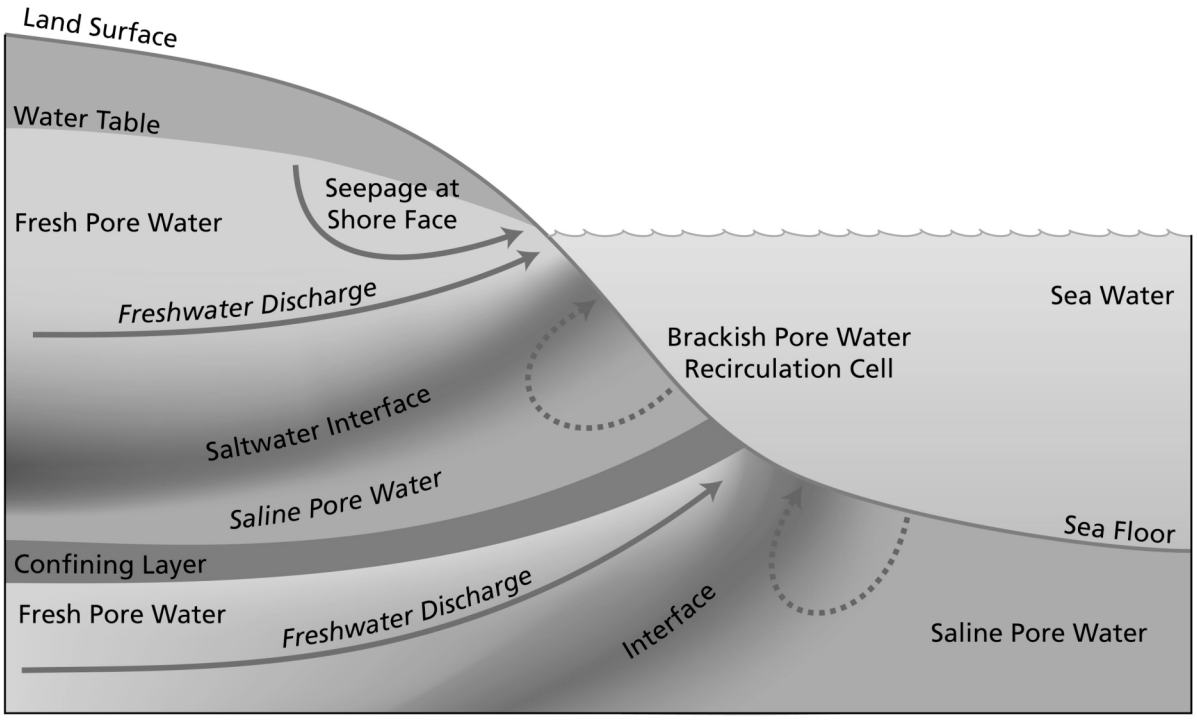
Land Surface
Water Table
Fresh Pore Water
Seepage at
Shore Face
Freshwater Discharge
Sea Water
Brackish Pore Water
Recirculation Cell
Saltwater Interface
Saline Pore Water
Sea Floor
Confining Layer
Fresh Pore Water
Freshwater Discharge
Interface
Saline Pore Water

Figure 1.

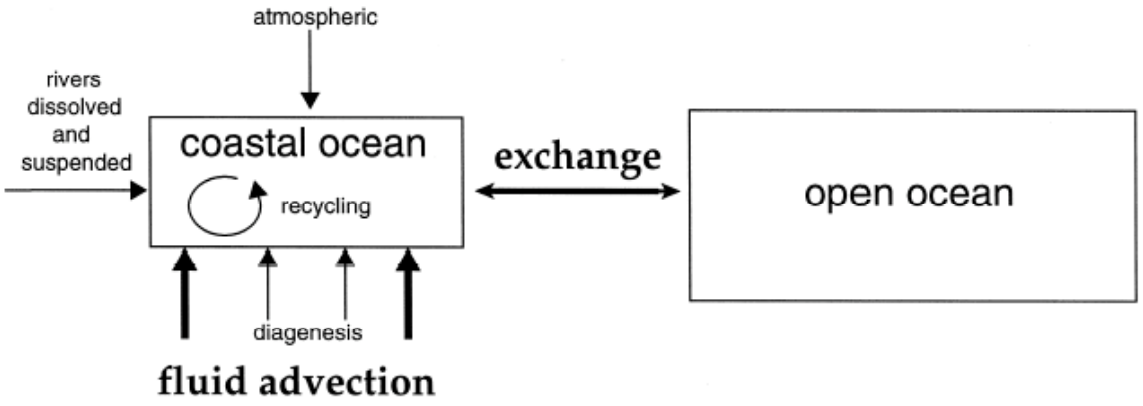
atmospheric
rivers
dissolved
and
suspended
coastal ocean
recycling
exchange
open ocean
diagenesis
fluid advection

Figure 2.

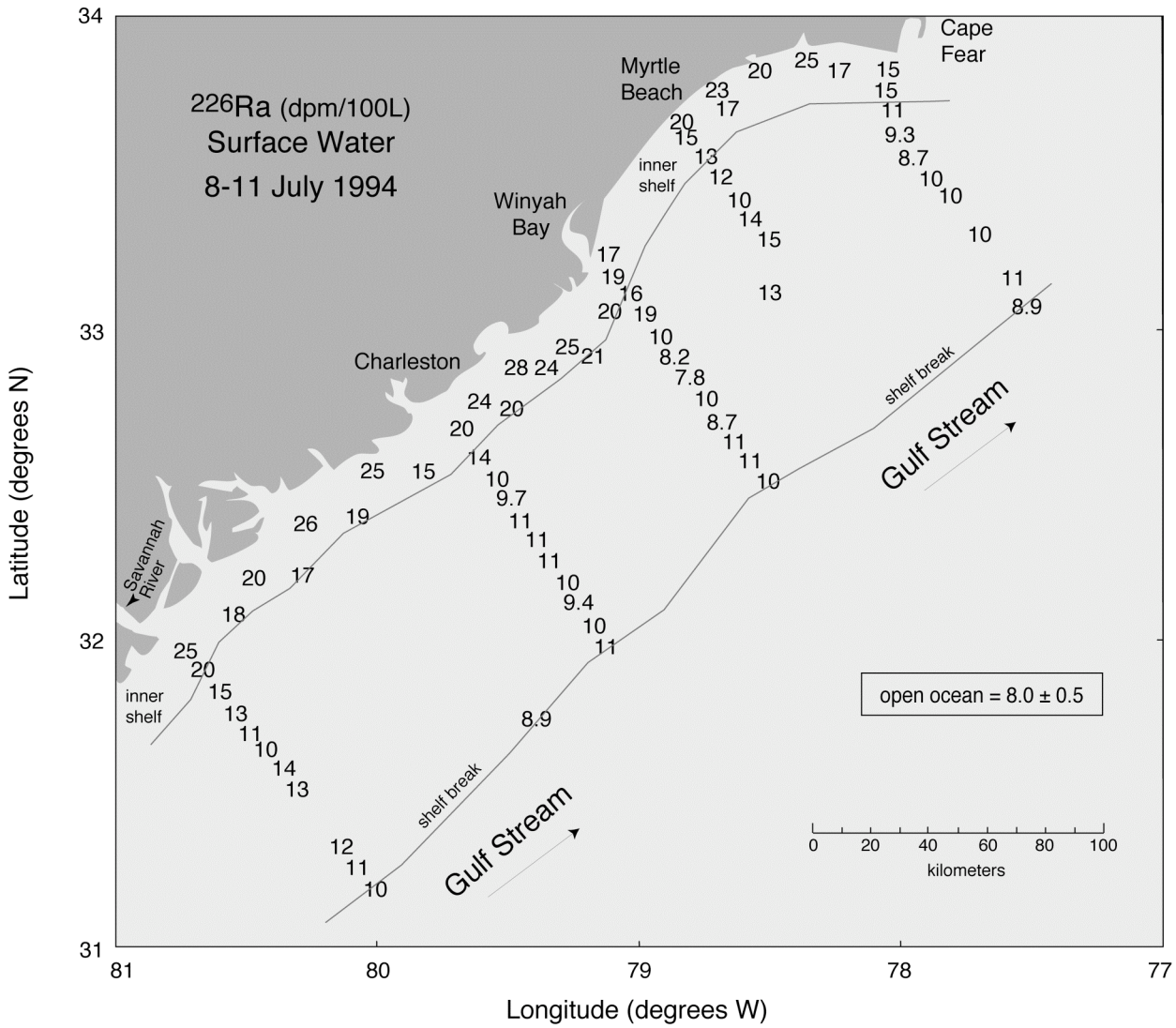
226Ra (dpm/100L)
Surface Water
8-11 July 1994
Cape Fear
Myrtle Beach
Winyah Bay
Charleston
Savannah River
inner shelf
shelf break
Gulf Stream
open ocean = 8.0 ± 0.5
0 20 40 60 80 100
kilometers
Latitude (degrees N)
Longitude (degrees W)
34
33
32
31
81
80
79
78
77

Figure 3.

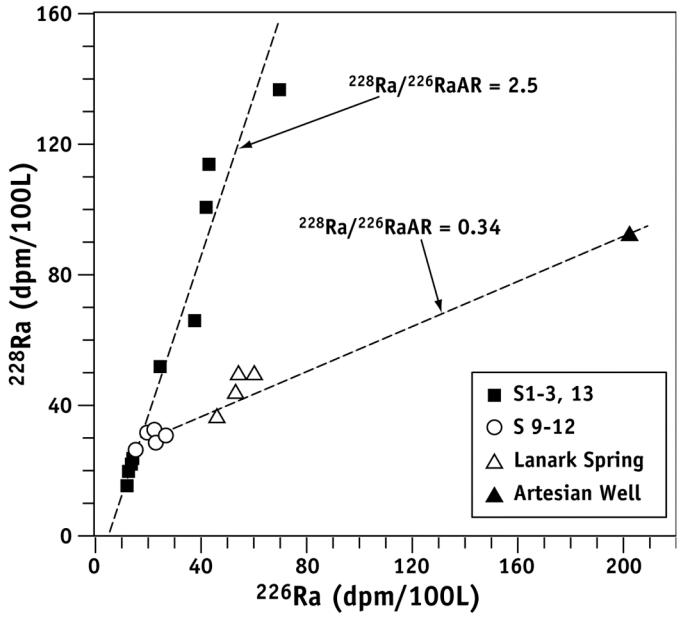
160
120
80
40
0
0
40
80
120
160
200
228Ra (dpm/100L)
226Ra (dpm/100L)
228Ra/226RaAR = 2.5
228Ra/226RaAR = 0.34
S1-3, 13
S 9-12
Lanark Spring
Artesian Well

Figure 4.

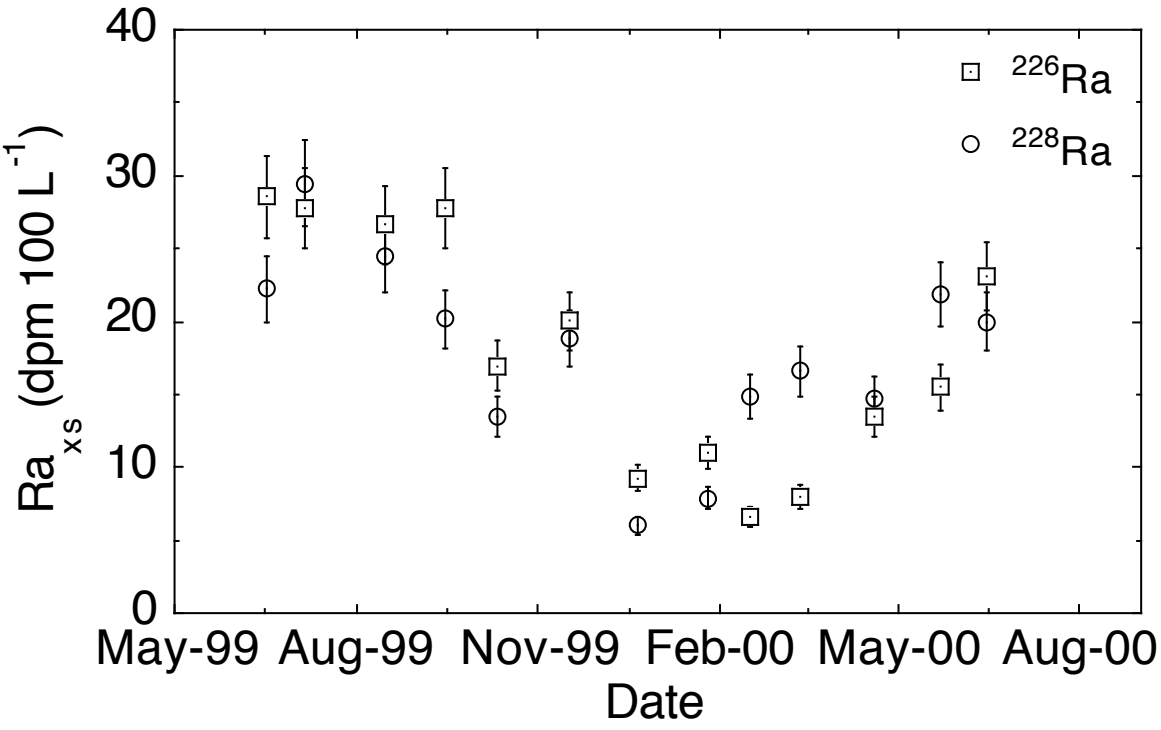
40
30
20
10
0
Ra_{xs} (dpm 100 L^{-1})
^{226}Ra
^{228}Ra
May-99
Aug-99
Nov-99
Feb-00
May-00
Aug-00
Date

Figure 5.

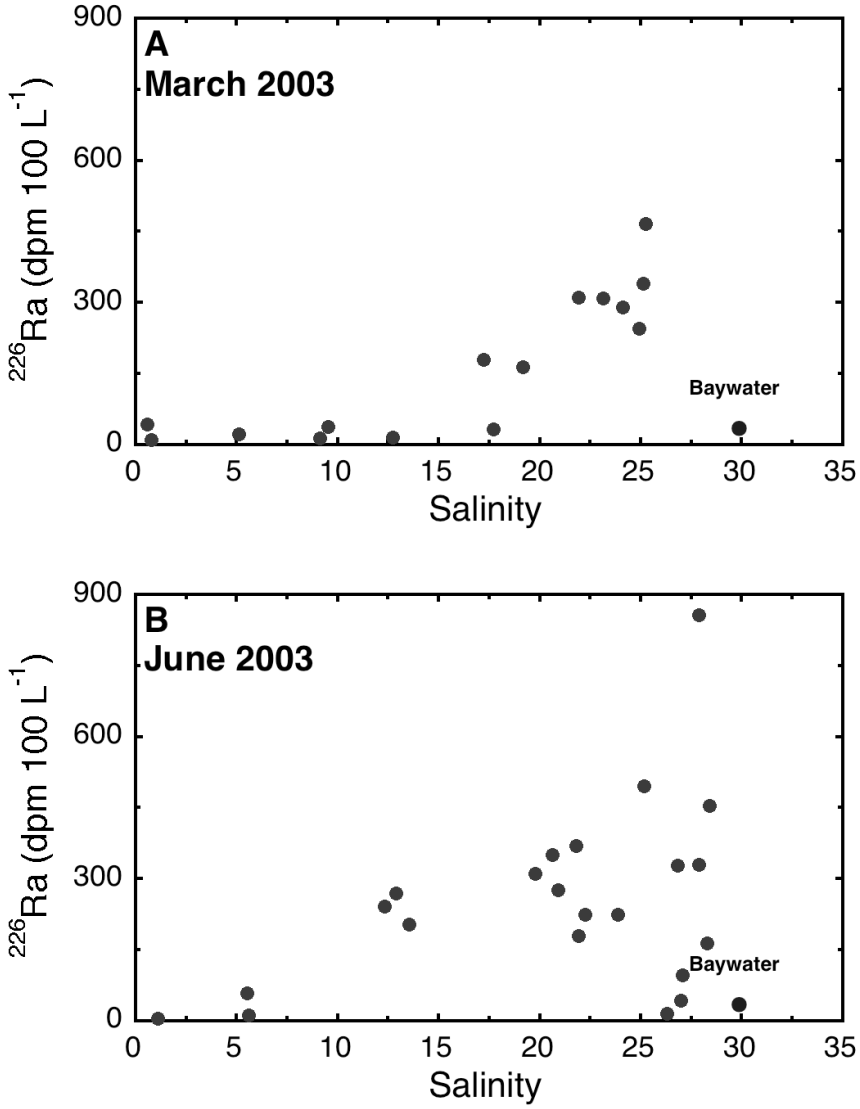
A
March 2003
^{226}Ra (dpm 100 L^{-1})
Salinity
Baywater
B
June 2003
^{226}Ra (dpm 100 L^{-1})
Salinity
Baywater

Figure 6.

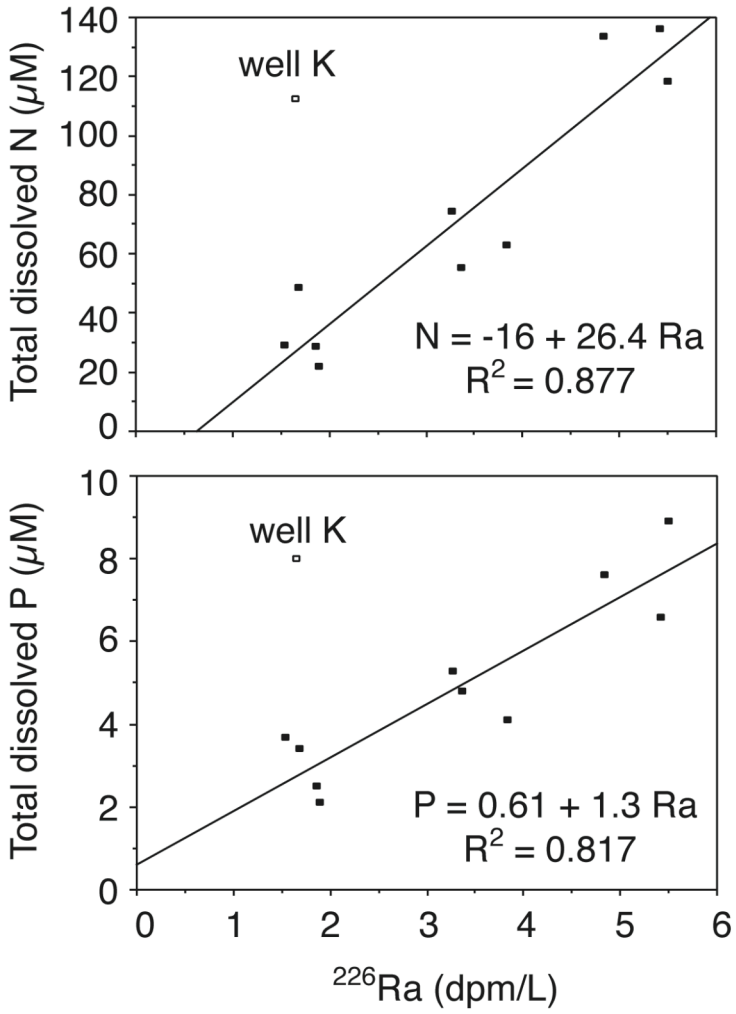
Total dissolved N (μM)
well K
N = -16 + 26.4 Ra
R2 = 0.877
Total dissolved P (μM)
well K
P = 0.61 + 1.3 Ra
R2 = 0.817
226Ra (dpm/L)

Figure 7.

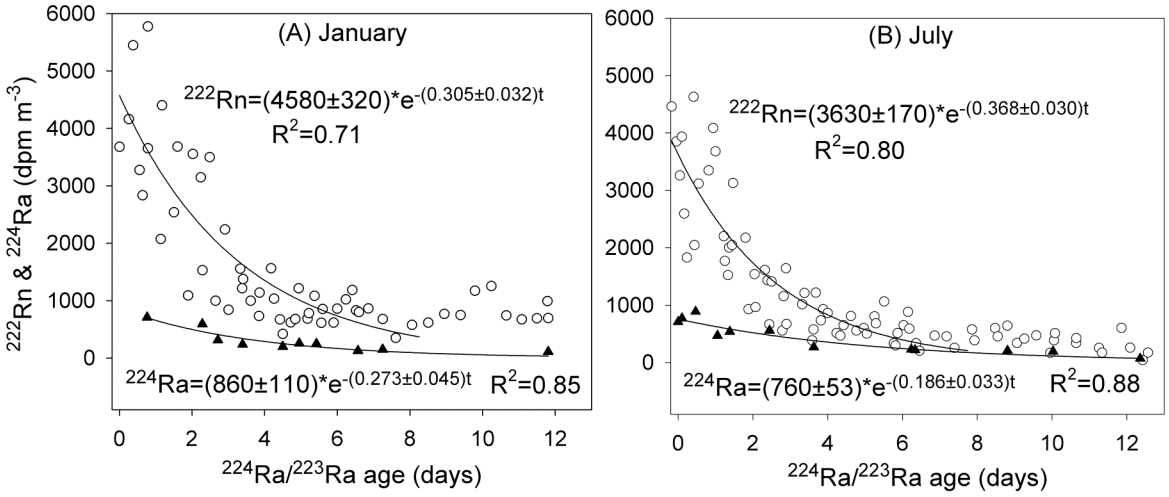
(A) January
$^{222}Rn=(4580\pm320)*e^{-(0.305\pm0.032)t}$
$R^2=0.71$
$^{224}Ra=(860\pm110)*e^{-(0.273\pm0.045)t}$ $R^2=0.85$
^{222}Rn & ^{224}Ra (dpm m^{-3})
$^{224}Ra/^{223}Ra$ age (days)
(B) July
$^{222}Rn=(3630\pm170)*e^{-(0.368\pm0.030)t}$
$R^2=0.80$
$^{224}Ra=(760\pm53)*e^{-(0.186\pm0.033)t}$ $R^2=0.88$
$^{224}Ra/^{223}Ra$ age (days)

Figure 8.

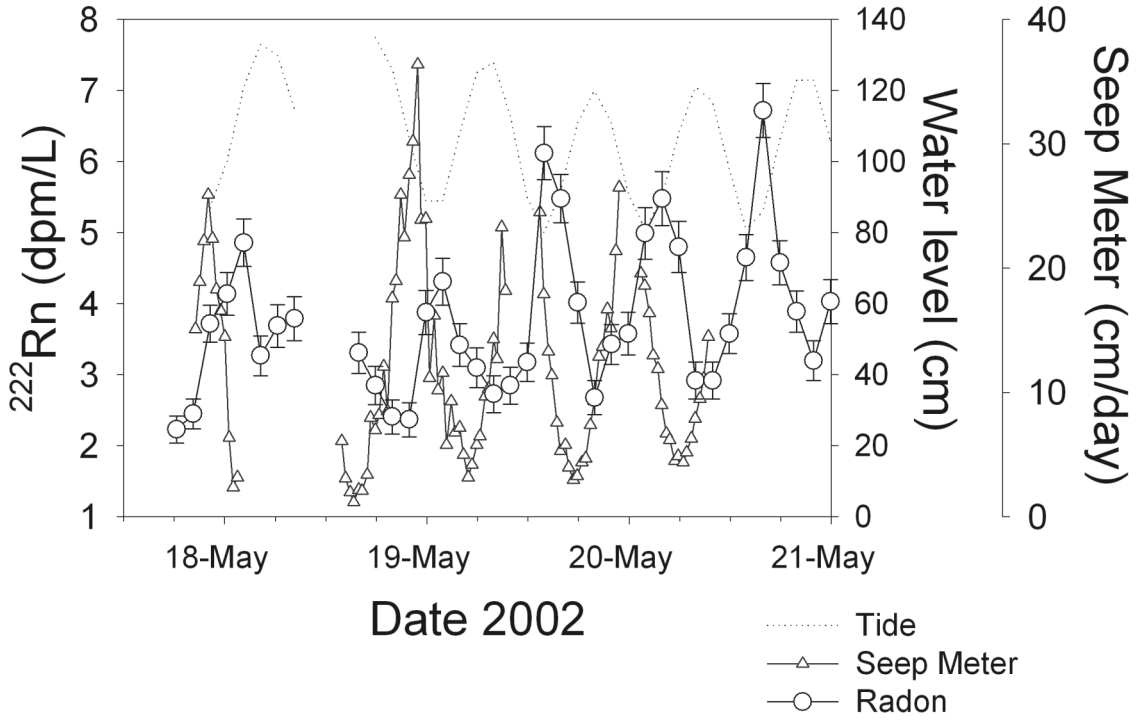
^{222}Rn (dpm/L)
Water level (cm)
Seep Meter (cm/day)
Date 2002
18-May
19-May
20-May
21-May
Tide
Seep Meter
Radon

Figure 9.

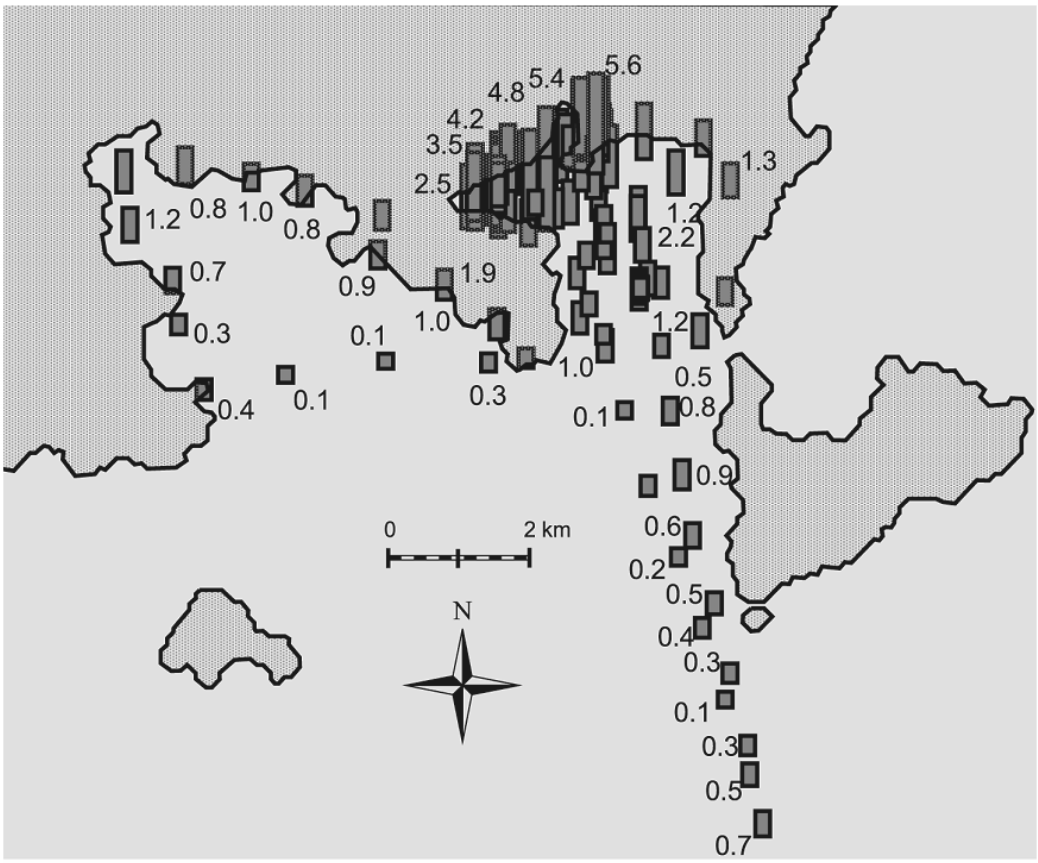
5.6
5.4
4.8
4.2
3.5
2.5
1.3
1.2
0.8
1.0
0.8
1.2
2.2
0.7
0.9
1.9
0.3
0.1
1.0
1.2
1.0
0.5
0.4
0.1
0.3
0.1
0.8
0.9
0
2 km
0.6
0.2
N
0.5
0.4
0.3
0.1
0.3
0.5
0.7

Figure 10.

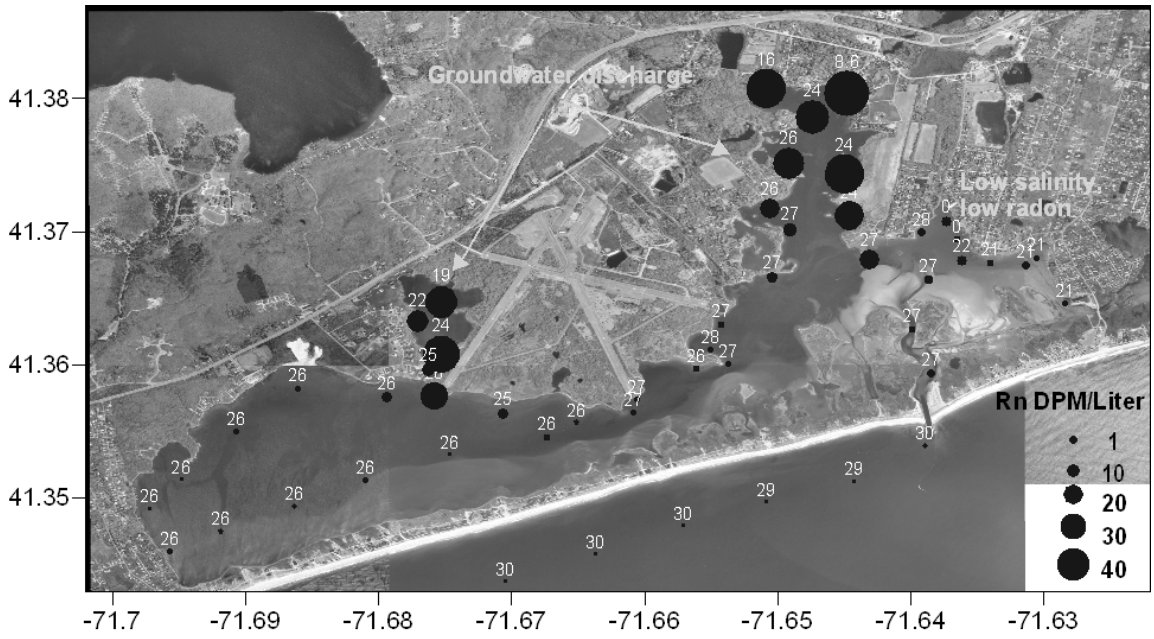
Groundwater discharge
Low salinity, low radon
Rn DPM/Liter
1
10
20
30
40
41.38
41.37
41.36
41.35
-71.7
-71.69
-71.68
-71.67
-71.66
-71.65
-71.64
-71.63

Figure 11.

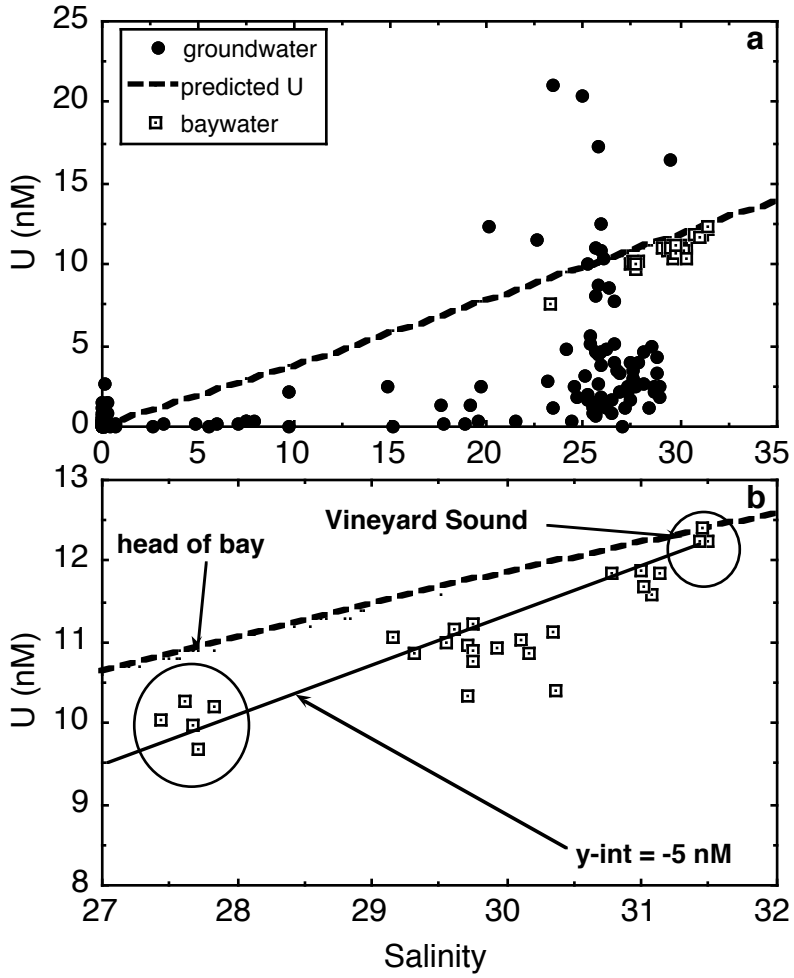
groundwater
predicted U
baywater
a
b
U (nM)
Salinity
head of bay
Vineyard Sound
y-int = -5 nM

Figure 12.

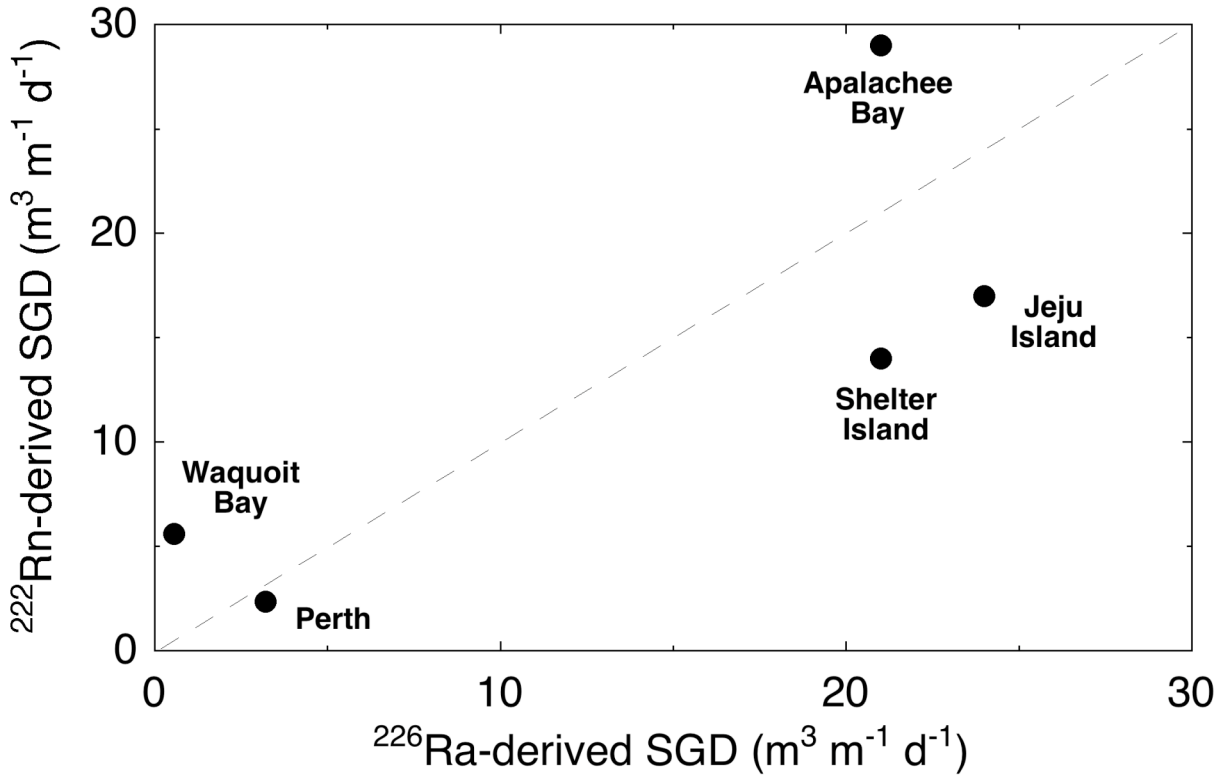
30
20
10
0
0
10
20
30
^{222}Rn-derived SGD (m^3 m^{-1} d^{-1})
^{226}Ra-derived SGD (m^3 m^{-1} d^{-1})
Apalachee Bay
Jeju Island
Shelter Island
Waquoit Bay
Perth

Figure 13.

Table 1. Shorline normalized fluxes from various Ra and Rn based SGD studies.

Flux ($m^3 m^{-1} d^{-1}$)	Location	Coastal Hydrogeologic Setting	Technique	Reference
Local-Scale Studies				
24	Jeju Island (Korea)	Basalt	^{226}Ra box model**	Hwang et al. (2005a)
17	Jeju Island (Korea)	Basalt	^{222}Rn box model***	Hwang et al. (2005a)
5-56	Flic en Flac (Mauritius)	Basalt	Continuous ^{222}Rn model****	Burnett et al. (2006)
5.3	Waquoit Bay, MA (USA)	Clastic	^{226}Ra box model	Charette et al. (2001)
9	Eckernförder Bay (Germany)	Clastic	^{222}Rn box model&	Purkl & Eisenhauer (2004)
12	Yeoja Bay (Korea)	Clastic	^{226}Ra box model#	Hwang et al. (2005b)
16-26	Shelter Island, NY (USA)	Clastic	^{226}Ra box model	Dulaiova et al. (2006a)
8-20	Shelter Island, NY (USA)	Clastic	Continuous ^{222}Rn model	Dulaiova et al. (2006a)
0.6-5.6	Waquoit Bay, MA (USA)	Clastic	Continuous ^{222}Rn model	Mulligan and Charette (2006)
200	Chao Phraya estuary (Thailand)	Clastic	Continuous ^{222}Rn model	Dulaiova et al. (2006b)
42-420	Pettaquamscutt Estuary, RI (USA)	Clastic/Fractured Igneous-Metamorphic	^{226}Ra box model##	Kelly and Moran (2002)
19-24	Huntington Beach, CA (USA)	Fractured Igneous-Metamorphic	^{226}Ra box model	Boehm et al. (2006)
11	Flamengo Bay (Brazil)	Fractured Igneous-Metamorphic	Continuous ^{222}Rn model###	Burnett et al. (2006)
21	Apalachee Bay, FL (USA)	Limestone	^{226}Ra box model	Burnett et al. (2002)
24-35	Apalachee Bay, FL (USA)	Limestone	Continuous ^{222}Rn model	Burnett et al. (2002)
3.2	Cockburn Sound, Perth (Australia)	Limestone	^{226}Ra box model	Burnett et al. (2006)
2.0-2.7	Cockburn Sound, Perth (Australia)	Limestone	Continuous ^{222}Rn model	Burnett et al. (2006)
30-200	Sicily (Italy)	Limestone	Continuous ^{222}Rn model	Burnett and Dulaiova (2006)
Regional-Scale Studies				
660-6,600	Bay of Bengal	Clastic	^{226}Ra/Ba box model	Moore (1997)
91-1500	Yellow Sea (China/Korea)	Clastic	^{226}Ra box model**	Kim et al. (2005)
94	South Atlantic Bight (US)	Clastic/Limestone	^{226}Ra box model	Moore (1996)
110	Coastal Brazil	Fractured Igneous-Metamorphic	^{226}Ra box model	Moore and Olivera (submitted
620-2,450	NE Gulf of Mexico	Limestone	^{222}Rn subpycnocline model*	Cable et al. (1996)
1000	Sicily/Mediterranean (Italy)	Limestone	^{226}Ra box model	Moore (2006)
Global Averages				
11	Terrestrial Groundwater	N/A	Combined hydrological-hydrogeological model	Zektser (2000)
5.34	Intertidal Pump	N/A	Direct measurements/theoretical model	Riedl et al. (1972)
437	Subtidal Pump	N/A	Direct measurements/theoretical model	Riedl et al. (1972)

*assumed shoreline length of 25 km
**assumed shoreline length of 1200 km
***assumed seepage face width of 50 m
#assumed seepage face width of 50 m
&assumed shoreline length of 16 km
##assumed shoreline length of 20 km
****range includes estimates from a local spring discharge